Proterozoic ophiolites from Yanbian and Shimian (Sichuan Province, China): petrography, geochemistry, petrogenesis, and geotectonic environment

by *Chuan Min Sun*[1,2] and *Marc Vuagnat*[1]

Abstract

The Middle Proterozoic ophiolites from the Yanbian and Shimian areas (Sichuan Province, China), which occur as allochthonous fragments embedded within the Late Proterozoic orogenic belt on the western rim of the Yangtse Craton, consist of mantle-derived tectonite peridotites, plutonic cumulates, and submarine volcanics.

The mantle sequence is made up of serpentinized harzburgites, representing an impoverished residual material after a high degree partial melting of upper mantle (> 30%). The plutonic sequence comprises ultramafic cumulates, Mg-gabbros (troctolites, Ol-anorthosites and Ol-gabbros), gabbronorites (including Ol-free gabbros), ferrogabbros, and albitites. The volcanic sequence consists of massive basalts with "sheet-flow" textures, pillowed basalts with associated hyaloclastites, and small amounts of ferrobasalts and keratophyres. This sequence is injected by sills and two types of dikes (dikes I and dikes II). Pelagic sediments occur as intercalations and cover of the volcanic piles.

Two magmatic suites are present. Suite I includes all the plutonic rocks and the great majority of volcanic and hypabyssal rocks. These rocks are characterized by an early crystallization of plagioclase prior to clinopyroxene and comparable to those from N-type Mid-Ocean Ridges. Such a magma would have been the liquid derived by a low degree partial melting (about 15%) from a slightly depleted mantle, and then submitted to a differentiation at low pressure (< 5 kb). In contrast, suite II is only represented by the dikes II, which are characterized by an early appearance of clinopyroxene as phenocrysts, and chemically comparable to plume-type MORB. This magma would have been derived from an enriched mantle also by a low partial melting (about 15%), undergoing later a differentiation at a relatively higher pressure (> 5 kb). None of the two suites can be considered as representing the liquid extracted from the studied peridotites. Using the 1-atm pseudo-quaternary system Ol-Pl-Di-Q and the distribution coefficient between mineral and liquid, the formation ranges of different plutonic rocks and the magmatic correspondence between plutonic and the suite I volcanic rocks are also determined.

Comparing with the characteristics of different present-day oceanic environments, it is likely that the Yanbian and Shimian Proterozoic ophiolites represent oceanic remnants which might have been formed at hot-spot-influenced spreading centers of small incipient oceanic basins, such centers being probably located in the vicinity of transform faults. The similarity of these ophiolites with present-day oceanic rocks indicates that the modern plate-tectonic processes may already have been active as early as Middle Proterozoic time.

Keywords: Proterozoic, ophiolites, petrography, geochemistry, petrogenesis, geotectonic environment, Sichuan, China.

Introduction

In contrast to the intensive geological, petrological and geochemical investigations of Phanerozoic ophiolites, only a few data on Precambrian ophiolites have been published recently (LE-BLANC, 1976; BODINIER et al., 1984; HARPER, 1985; KONTINEN, 1987; BERHE, 1990; DANN, 1991). Since ophiolites represent the remnants of ancient oceanic lithosphere, studies of Precambrian ophiolites can provide some important informations on the characteristics of oceanic crust and mantle composition of that time.

Two Proterozoic ophiolitic complexes are studied in this paper: one is situated in the Yanbian and the other in the Shimian area (Fig. 1). The

[1] Département de Minéralogie, Université de Genève, 13, rue des Maraîchers, CH-1211 Genève 4, Switzerland.
[2] Department of Geology, Chengdu College of Geology, Chengdu, Sichuan 610059, China.

Yanbian Proterozoic ophiolite complexes have been known for some time (GEOLOGICAL TEAM 106, 1975; LI et al., 1983; LI, 1984; LAI, 1983; ZEN, 1985), but their petrogenetic and geotectonic nature was ambiguous. The Shimian ophiolites have been mentioned only in one report (ZEN et al., 1982) and their origin was even less clear. Recently, it has been proved that the ophiolites located in the two areas mentioned above appear in the same orogenic belt with the same affinity, comparable to the Phanerozoic high-Ti ophiolites (SUN, 1990), so they can be called Yanbian-Shimian Proterozoic ophiolites (YSPO). A detailed geochemical study of the clinopyroxenes of the plutonic and volcanic rocks of the Yanbian ophiolites also showed a good similarity to typical high-Ti Phanerozoic ophiolites (SUN and BERTRAND, 1991). In this paper, new petrographic and
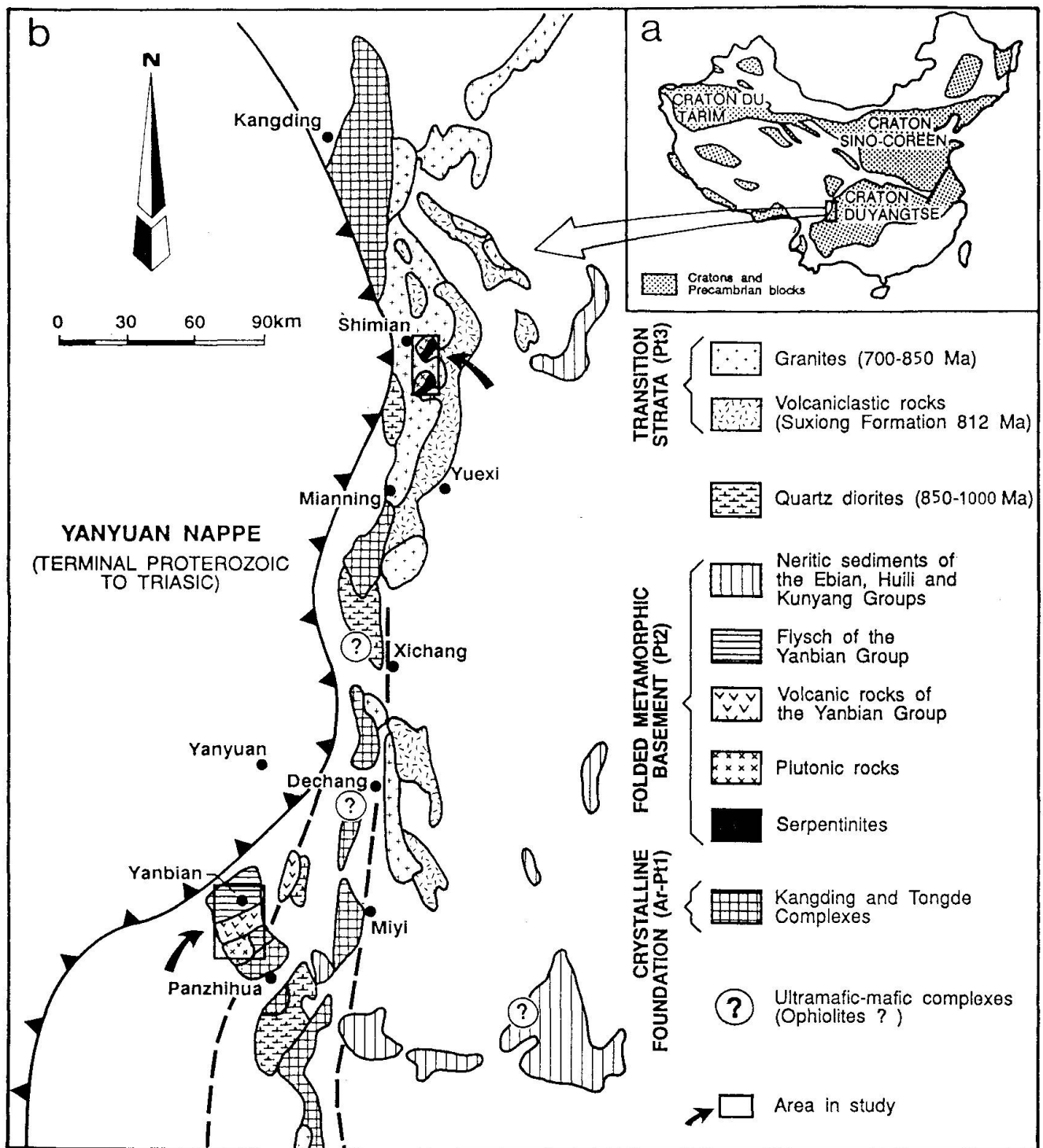

Fig. 1 Simplified geological map of the Late Proterozoic orogenic belt on the western rim of the Yangtse Craton.

geochemical data are presented. Using trace element data and a 1-atm Ol-Pl-Di-Q system, the petrogenetic processes are discussed; finally, comparing with different present-day oceanic tectonic settings, a possible geotectonic environment for the YSPO is also proposed.

1. General geological framework

On the western rim of the Precambrian Yangtse Craton (ZHANG et al., 1984) there is a Late Proterozoic orogenic belt extending from north to south for about 700 km, which comprises the following units (Fig. 1):

(1) Crystalline basement (Archean to Early Proterozoic), consisting of amphibolites, gneisses, migmatites, and granulites, intruded by Late Proterozoic quartz-diorites.

(2) Folded metamorphic basement (Middle Proterozoic), composed of meta-volcano-sedimentary rocks in greenschist facies. This terrane can be subdivided into two zones, separated by N–S oriented blocks of unit (1). The eastern zone is characterized by neritic meta-sedimentary rocks with intercalations of bimodal volcanic and volcano-detritic rocks (alkaline basalts, rhyolites, and trachyandesites). The western zone, occurring mainly in the Yanbian area, is characterized by flysch formations in which ophiolitic submarine volcanics, pelagic sediments and plutonic rocks are embedded.

(3) "Transition strata" (Late Proterozoic), overlying discordantly the units (1) and (2), and made up of intermediate and acid volcanic and volcano-detritic rocks intruded by S-type granites.

All these units are overlain discordantly by a platform type sedimentary cover of late Proterozoic to Cambrian age.

The Yanbian ophiolites consist of submarine volcanics (1006 + 58 Ma, Rb–Sr; LI et al., 1983) with pelagic sedimentary intercalations and of plutonic cumulates (1253, 1112 Ma, K–Ar; GEOLOGICAL TEAM 106, 1975), occurring as huge allochthonous fragments embedded within the flysch formations in the western zone of unit 2. The large discrepancies of ages may be due to analytical errors and post-magmatic metamorphism. It is likely that the measured age for the volcanics represents that of metamorphism. As the plutonic rocks have high crystallinity and are less metamorphosed, their measured ages may approach the ages of the ophiolites. The Shimian ophiolites are mainly composed of serpentinites and plutonic cumulates, exposed as tectonic slices overlain discordantly by the unit (3) whose age was determined to be 812 ± 16 Ma (Rb–Sr; LUO, 1988). Although the studied ophiolites have been dismembered and metamorphosed into greenschist facies, the three characteristic sequences of ophiolite can be recognized: mantle-derived tectonite peridotites, plutonic cumulates, and submarine volcanics. However, no sheeted-dike complex has been found (Fig. 2).

2. Petrography

2.1. MANTLE-PERIDOTITES

The mantle sequence crops out as two tectonic slices situated a few kilometres south of Shimian. It is represented by serpentinites cross-cut by albitite and dolerite dikes; the latter were transformed into typical rodingites, forming in some places rounded "ophispherites" like those described in the Alps (VUAGNAT, 1952, 1953, 1954). In handspecimen, the serpentinites exhibit three structures: massive, foliated, and mottled, but in thin sections, the mineral assemblage is monotonous. Despite a strong degree of serpentinization (to about 90% antigorite and chrysotile), some relics of olivine (Ol) (Fo_{96-97}), enstatite (En), and chromian spinel (Cr-Sp) are found. The rocks are medium grained (0.5–4 mm), and have porphyroclastic and granoblastic structure. Some of these relics exhibit wavy extinction and kink-bands. Accessory red-brown Cr-Sp occurs randomly in interstitial spaces at Ol and Opx (orthopyroxene) grain boundaries and their shape is similar to the "holly leaf" texture described in some mantle-derived peridotites (MERCIER and NICOLAS, 1975; NIELSON and SCHWARZMAN, 1976). These features are characteristic of upper mantle peridotites which have been submitted to strong plastic deformation, and probably, comparable to the transitional subtype between the "ridge coarse texture" and the "trench fine porphyroclastic structure" attributed to the "fracture zone" (NICOLAS et al., 1980).

2.2. PLUTONIC SEQUENCE

This sequence occurs both in the Shimian and the Yanbian areas, but is better exposed in the latter locality. It consists of a differentiation succession, represented by the following rock types: (1) ultramafic cumulates, (2) Mg-gabbros, (3) gabbronorites, (4) ferrogabbros, and (5) albitites. The layering, which is accentuated by the variations in colour and grain size, can be observed at outcrops of the first three types. Gabbroic pegmatites and

doleritic dikes are also present in the plutonic sequence.

The ultramafic cumulates, including Pl- (plagioclase) dunites and Pl-lherzolites, occur as tabular layers within the gabbronorites and gabbros. They are characterized by Ol (Fo_{81-82}) and Cr-Sp as cumulus phases, with Pl (plagioclase, An_{76}), a few Cpx ($Wo_{44.5-47.4}En_{43.0-45.2}Fs_{9.1-10.5}$), and Opx ($En_{83.0-83.5}$) as intercumulus phases, displaying a mesocumulus texture. In some places, Cu–Fe–Ni ore pockets (pentlandite-pyrrhotite-pyrite) are present in the basal part of the ultramafic rocks.
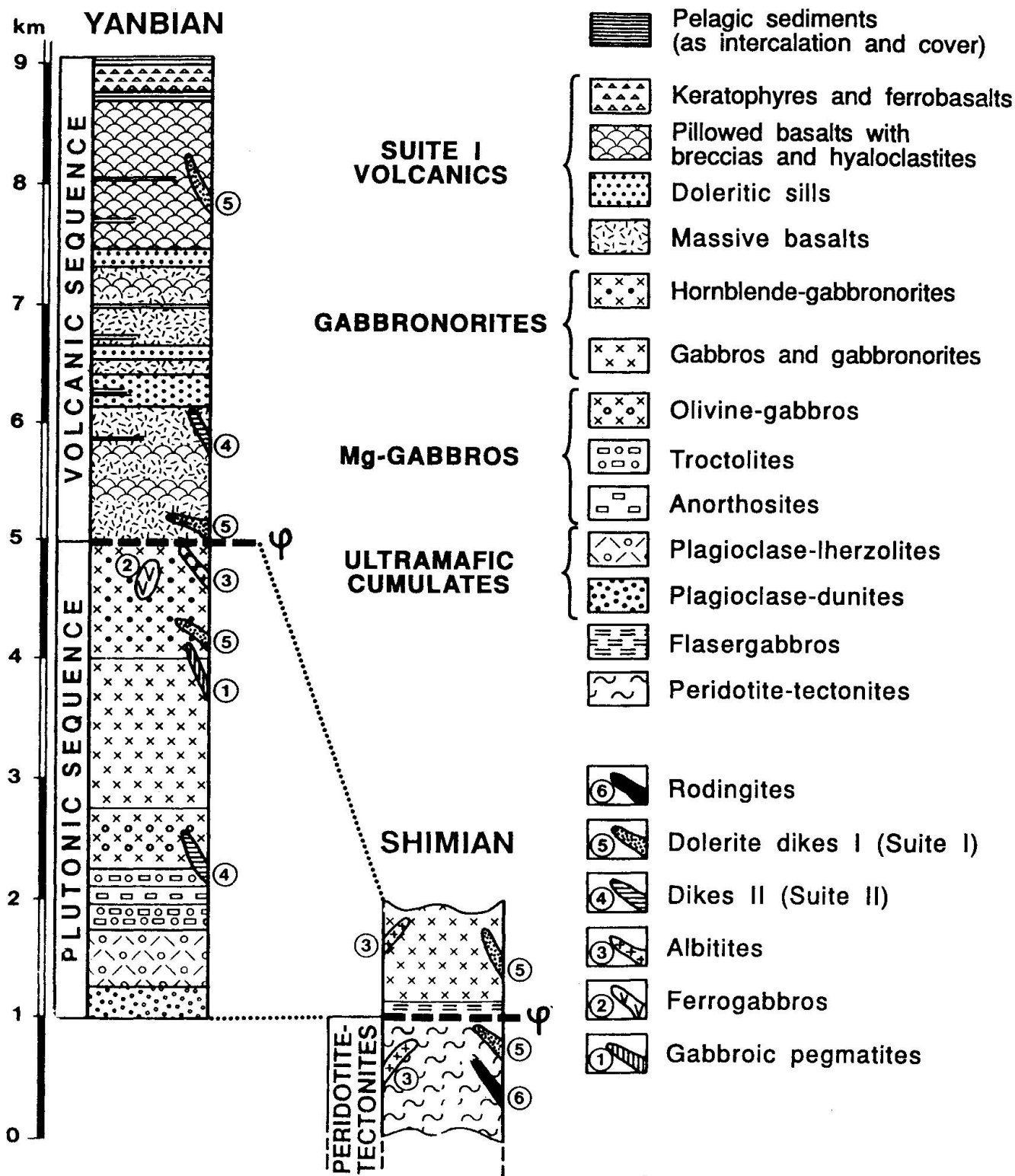

Fig. 2   Reconstruction of the Yanbian-Shimian Proterozoic ophiolite (YSPO) series.

The Mg-gabbros, located in the transition zone between the ultramafic cumulates and the gabbronorites, comprise troctolites, Ol-anorthosites, and Ol-gabbros, exhibiting adcumulus texture. The troctolites and Ol-anorthosites are mainly composed of cumulus Ol ($Fo_{81.6-82.9}$) and Pl (An_{70-72}), and of minor intercumulus Cpx. The Ol-gabbros consist of cumulus Ol ($Fo_{78.2-78.9}$), Pl (An_{65}), and Cpx ($Wo_{45.3-47.47}En_{43.0-45.2}Fs_{10.0-12.4}$). Opx (enstatite) are very rare in these rocks and sometimes forms a thin envelope around Ol grains. The gabbronorites, which include also Ol-free gabbros, are characterized by Pl (An_{56-65}) and Cpx ($Wo_{37.4-47.9}En_{38.5-45.2}Fs_{11.9-17.4}$) as cumulus phases, with Hyp (hypersthene $En_{70.0-71.9}$), brown Hbl (hornblende) as well as Ap (apatite) and Ti-Mt (titanomagnetite) as intercumulus phases, showing heteradcumulus texture. The ferrogabbros, which are exposed as pods within the gabbronorites and gabbros, consist of Pl (An_{48}), Cpx ($Wo_{41.2-45.8}En_{38.5-40.7}Fs_{15.7-18.9}$), Hyp ($En_{65.2-67.5}$), and Ap as cumulus phases, and brown Hbl and Ti-Mt as intercumulus, displaying heteradcumulus texture. A few zircon crystals are observed in thin sections. The outcrops of the albitites are extremely rare, occurring as small dikes or veins within the gabbronorites and gabbros. They are made up of oligoclase (An_{17}) phenocrysts in a matrix of albite and scant quartz (Q); some crystals of zircon and allanite are also present.

These observations indicate therefore that the crystallization order throughout the plutonic sequence was as follows: Ol (in ultramafics); Pl (in Mg-gabbros); Cpx (in Ol-gabbros and gabbronorites); Opx; Ap+Ti-Mt; brown Hbl (in gabbronorites and ferrogabbros); zircon; Q (in albitites).

2.3. VOLCANIC SEQUENCE

The volcanic sequence is mainly exposed in the Yanbian area. It consists of massive basalts with a few pillows in the lower part of the section, variolitic pillowed basalts with hyaloclastites, breccias, and massive basalts in the upper part of the sequence, and minor keratophyres and ferrobasalts at the top. Pelagic sediments appear as intercalations or cover of the volcanic pile. Sills and dikes are also present.

The massive basalts show a bedded structure with thickness varying from a few centimetres to a few meters, similar to the sheet-flows described by BALLARD et al. (1979). They are mainly aphyric; some samples contain Ol and Pl phenocrysts. Fine-grained texture, often intersertal, dominates in thin bedded basalts. Coarse-grained texture

(ophitic to subophitic) is observed in thick bedded basalts. The primary minerals are strongly altered, only Cpx relics are preserved in some samples. In the coarse-grained basalts, the Cpx has an average composition of $Wo_{42.4}En_{41.0}Fs_{16.6}$ with 1.29% TiO_2 and 3.62% Al_2O_3. In the fine-grained basalts the average composition of the Cpx is $Wo_{43.7}En_{33.1}Fs_{23.2}$ with 2.17% TiO_2 and 4.27% Al_2O_3.

The pillow lavas, which have variable size (usually 40-80 cm), contain Pl (+Ol) phenocrysts and display a remarkable concentric structural zoning due to variation of cooling rate. From margin to core, the pillows exhibit the following variation of textures: variolitic; spherolitic; arborescent; divergent intersertal; intersertal. This succession is in agreement with that of the Alpine ophiolitic pillow lavas (VUAGNAT 1946; MEVEL, 1975) as well as some of present-day oceanic pillows (JUTEAU et al., 1980).

Only one outcrop of ferrobasalts has been found. These rocks occur as an irregular layered lens within the keratophyres. They are composed of Pl phenocrysts and microlites, interstitial secondary chlorite, and abundant Ti-Mt-derived sphene and leucoxene (> 10 vol.%). Some cubic sections (about 1 mm) of pseudomorphosed Tt crystals are observed under the microscope.

The keratophyres are Pl- (oligoclase and albite) and Q-rich rocks, containing oligoclase phenocrysts. The matrix is fine-grained, with trachytic texture. Some samples appear quite glassy, showing perlitic texture. Based on the classification of LE BAS et al. (1986), their overall chemical compositions correspond to low-K/high-Na andesite, trachyandesite, trachyte, and trachydacite. Their high contents in Y (> 70 ppm) and Zr (> 500 ppm) and low concentration in V (< 35 ppm) and Ba (< 9 ppm), as well as field relations (overlain by pelagic sediments), preclude both orogenic (subduction-related) and continental origin (GILL, 1981), but are comparable to those of oceanic plagiogranites (COLEMAN and PETERMAN, 1975).

The dolerite sills are concentrated in the lower part of the volcanic sequence, but they do not form a typical sheeted-sill complex between plutonic and volcanic sequences. In general these rocks have an ophitic to subophitic texture. In contact with the basalts, no chilled margins are visible.

The dikes can be subdivided into two groups. The first one (dikes I) cuts the majority of the plutonic and volcanic rocks, but does not inject the keratophyres at the top of the volcanic sequence. These dikes are strongly altered, but Ol and Pl phenocrysts remain recognizable. They show chilled margins in contact with the plutonic

Tab. 1a Major and trace element content ranges of the YSPO.

Rock types	MP(4)	UC(4)	MG–G TR+AN(2)	Ol–G(2)	GN(5)	FG(1)	AB(2)
SiO_2	39.82–41.05	38.01–41.83	42.26–44.81	42.53–45.28	44.53–47.24	40.61	56.65–61.66
TiO_2	80–0.02	0.16–0.53	0.10–0.21	0.22–0.36	0.64–2.33	4.62	0.10–0.12
Al_2O_3	0.54–1.23	5.03–8.76	25.61–27.38	10.50–24.50	12.45–19.78	15.25	21.04–25.87
Fe_2O_3	4.83–7.21	4.19–7.54	1.56–1.81	1.86–5.22	4.26–9.68	12.83	0.81–1.54
FeO	0.58–1.09	5.05–6.83	1.48–2.77	1.93–6.04	2.39–5.54	5.83	0.10–0.17
MnO	0.08–0.12	0.17–0.26	0.05–0.06	0.06–0.18	0.14–0.22	0.25	0.01
MgO	39.27–40.15	23.31–32.03	4.87–9.02	6.64–18.13	4.14–14.95	5.63	0.12–0.26
CaO	0.02–0.08	2.18–4.90	13.16–15.03	11.31–15.63	9.34–1.41	9.94	3.78–7.81
Na_2O	0.02–0.11	0.17–0.86	1.04–1.26	0.63–1.22	1.04–3.96	2.10	6.39–8.44
K_2O	0–0.01	0.04–0.13	0.06–0.11	0.05–0.17	0.11–0.35	0.21	0.20–1.10
P_2O_5	0	0.04–0.13	0.02–0.03	0.01–0.03	0.05–0.84	0.80	0.05
H_2O+	12.12–12.41	4.76–11.17	2.99–3.50	1.77–4.76	0.74–1.63	1.11	0.55–0.75
CO_2	0–0.23	0–0.43	0.06–0.37	0.29–0.38	0–0.59	0	0–0.11
Total	99.96–100.49	99.9–100.07	99.44–99.54	99.58–99.67	99.20–99.88	99.18	98.08–99.61
Hf	n.d	1–2	2	2	2–5	2	5
Ba	n.d	70–117	59	n.d	n.d	–	–
Rb	n.d	2–6	3–11	2–43	2–11	5	2
Sr	n.d	113–329	769–1159	349–1159	432–1159	671	1515
Y	n.d	5–8	5–8	5	5–44	20	10
Zr	n.d	6–26	n.d	2	7–249	220	144
V	23–26	79–192	20–80	88–150	139–304	650	14–26
Cr	1853–2162	1993–4174	169–569	507–1192	2–57	199	37–81
Ni	2332–2525	432–960	110–156	121–298	4–161	18	8–34
Co	85–96	101–166	11–54	20–96	34–91	74	42–86
Cu	4–9	21–60	41–42	44–50	18–45	17	2–8
Zn	29–40	94–131	23–56	23–80	60–153	130	19
FeO*	5.44–7.07	9.35–13.51	3.16–4.17	3.60–10.74	7.86–12.38	17.38	0.9–1.49
F/M	0.13–0.17	0.28–0.58	0.47–0.66	0.56–0.61	0.81–2.57	3.16	3.46–13.28
F/F+M	0.12–0.15	0.22–0.37	0.32–0.40	0.36–0.38	0.45–0.72	0.76	0.78–0.93
Zr/Y		1.20–3.25		2.50	1.42–5.65	11.00	14.4

Data analyzed by XRF at the geochemical laboratory of the Department of Mineralogy, University of Geneva; (Nb at the laboratory of C.N.R.S, Vandoeuvre, France). MP = mantle peridotite; UC = ultramafic cumulate; Mg–G = Mg–gabbros; TR = troctolite; AN = anorthosite; Ol–G = Ol–gabbro; GN = gabbronorite; FG = ferrogabbro; AB = albitite; MB = massive basalt; PB = pillowed basalt; SIL = sill; DI = dikes I; D.II = dikes II; FB = ferrobasalt; KER = keratophyre. F/M = FeO*/MgO; F/F+M = FeO*/(FeO*+MgO); (n) = number of analyzed samples.

rocks, but no chilled margins against the basaltic rocks. Dikes of the second group (dikes II) are less altered, cross-cutting all the rock types and displaying sharp chilled margins against the surrounding basaltic rocks. These dikes are mainly of basaltic composition, some of them are picritic. They contain Cpx phenocrysts of variable compositions due to different cooling rates. The large Cpx phenocrysts (1.5–2 mm) have an average composition $Wo_{40.5}En_{32.6}Fs_{26.9}$ with 0.75% TiO_2 and 1.46% Al_2O_3, whereas the small phenocrysts (0.5 mm) have an average composition $Wo_{41.4}En_{43.8}Fs_{14.8}$ with 1.78% TiO_2 and 5.00% Al_2O_3.

The pelagic sediments comprise meta-siltstone, shale, mudstone, and notably chert, some lenses of Fe-Mn-rich sediments are also present. The sediments appear more abundant in the basal part of the volcanic sequence, and in contact with sills and dikes I, some bleached "adinoles" (AGRELL, 1939) can be observed. This phenomena has also been found in Alpine ophiolite-related pelagic sediments, as described by VUAGNAT (1946).

The lack of chilled margins in contacts between basalts, sills, and dikes I, as well as their similar compositions (see later) suggests that the sills and dikes I were the magma-conduits of the

Tab. 1b Major and trace element content ranges of the YSPO.

Rock types	MB(5)	PB(5)	SIL(2)	DI(2)	DII(6)	FB(2)	KER(4)
SiO_2	45.99–50.81	39.33–52.13	46.71–49.15	44.18–45.12	45.53–52.98	38.00–40.59	59.19–70.50
TiO_2	1.66–1.84	0.38–2.06	1.91–3.47	0.99–2.50	0.89–2.81	2.14–2.17	0.66–1.54
Al_2O_3	12.58–15.44	13.02–15.47	11.80–13.99	14.05–19.15	8.31–15.55	14.76–14.97	10.06–17.98
Fe_2O_3	3.81–5.68	2.76–6.80	3.77–7.54	4.56–7.15	1.57–5.15	3.32–4.93	1.40–3.27
FeO	5.24–9.31	5.31–11.75	6.47–8.69	2.92–9.29	6.12–11.89	19.87–20.86	4.91–6.72
MnO	0.15–0.20	0.17–0.26	0.23–0.24	0.15–0.30	0.15–0.39	0.31–0.33	0.16–0.34
MgO	4.20–8.56	5.49–8.78	4.70–6.67	4.59–6.95	2.22–18.25	3.27–3.72	0.98–1.36
CaO	9.27–11.38	8.58–13.74	8.93–10.22	9.32–14.70	5.98–10.20	3.50–3.64	0.57–4.13
Na_2O	1.98–3.06	0.09–2.52	2.81–3.92	1.88–2.53	1.40–3.68	1.93–2.25	3.87–8.62
K_2O	0.15–0.49	0.07–0.58	0.28–0.41	0.15–0.16	0.38–2.77	0.69–0.81	0.25–0.92
P_2O_5	0.19–0.25	0.04–0.27	0.28–0.41	0.14–0.34	0.20–0.87	0.83	0.16–0.77
H_2O+	2.41–3.57	1.81–5.82	2.27–3.00	2.70–3.46	1.51–3.26	6.80–6.99	2.34–2.51
CO_2	0.43–0.68	0.82–3.04	0.52–0.69	0.62–0.73	0.33–0.90	0.33–0.39	0–1.52
Total	99.32–99.79	99.08–99.71	99.38–99.70	99.31–99.32	99.18–99.99	99.08–100.15	99.98–100.70
Hf	2–4	1–4	3–5	2–3	3–9	19	13–36
Ba	137–249	107–243	251–304	113–137	198–1641	n.d	126–624
Rb	1–10	5–18	4–6	4–6	11–46	10–12	1–9
Sr	255–420	240–683	225–250	357–2097	166–833	129–155	96–245
Y	31–46	24–44	37–60	17–41	16–138	194–213	70–109
Zr	85–171	63–161	114–216	48–143	95–977	1257–1160	558–1598
V	277–408	167–404	381–520	202–444	54–346	74–86	15–35
Cr	141–289	43–217	238	86–236	1–1271	5–6	6–11
Ni	31–155	45–76	7–47	52–65	3–679	11–12	4–9
Co	47–62	45–66	48–51	40–52	45–70	79–89	18–22
Cu	55–90	39–104	7–94	12–89	7–151	2–4	5–12
Zn	78–105	75–122	78–94	92–110	85–198	300–312	142–198
Nb	5	5	5	6	22	n.d	20
FeO*	10.35–12.74	9.33–15.13	12.08–13.26	9.36–13.39	7.80–14.08	22.86–25.30	7.34–8.87
F/M	1.22–2.44	1.69–2.14	1.81–2.82	1.93–2.03	0.66–6.32	6.80–6.99	5.46–8.14
F/F+M	0.55–0.71	0.63–0.68	0.64–0.74	0.66–0.67	0.40–0.86	0.87–0.88	0.85–0.89
Zr/Y	2.74–3.80	2.43–3.66	3.08–3.60	2.82–3.49	5.94–9.00	5.45–6.48	7.48–14.66

basalts. The fact that the dikes I cross-cut the plutonic rocks with chilled margins and that the sedimentary intercalations contain plutonic-derived fragments suggests that the effusion of the volcanics was posterior to the plutonic sequence. Such a non-contemporaneous relationship between plutonic and volcanic sequences has been observed in ophiolites of the Western Alps. (BERTRAND et al., 1987).

2.4. ALTERATION AND METAMORPHISM

Careful microscopic examination shows that two post-magmatic processes affected the ophiolites: regional metamorphism and pre-regional metamorphism alteration. The former is present in the great majority of volcanic and associated sedimentary rocks and characterized by the "recrys-

tallization" in the parageneses of greenschist facies with a strong foliation. The pre-regional metamorphism, which can be recognized only in some samples of magmatic rocks, is characterized by "alteration" of primary minerals and by "infilling" of primary cavities, such as vesicles and cooling cracks of pillow lavas, with non-aligned fabric. It is interesting to note that some of the "alteration" mineral assemblages vary regularly from bottom to top of the ophiolite succession. For instance, green Hbl is present in the plutonic sequence, green-blue Hbl in the lower part of the volcanic sequence, and pumpellyite and prehnite in the upper part and at the top of the volcanic sequence. This variation reflects a regular decrease of transformation temperature through the ophiolitic succession. These features correspond to the characteristics of "oceanic metamorphism" observed both in the Phanerozoic ophiolites and

Tab. 2   Rare-earth element (REE) concentrations of the YSPO volcanic rocks (in ppm).

Sample	S-11 1	S-24 2	S-12 3	S-28D 4	S-27 5	S-3 6	S-90 7	S-55 8	S-37 9	Chondrite values
La	5.27	9.36	4.07	7.49	8.51	9.60	27.30	26	46.26	0.329
Ce	23.25	41.29	14.49	29.05	37.37	44.99	70.42	53	112.15	0.865
Nd	12.76	18.69	10.35	16.95	16.54	20.20	33.64	n.d	102.90	0.630
Sm	4.38	5.96	3.69	5.31	4.95	6.53	7.87	9.7	16.61	0.203
Eu	1.44	1.98	1.37	1.94	1.75	2.22	2.35	2.0	4.69	0.077
Gd	4.87	6.87	4.90	6.34	5.87	7.47	7.84	n.d	16.25	0.276
Dy	5.09	7.07	4.54	7.09	6.25	7.37	5.59	n.d	18.31	0.343
Er	2.76	3.98	2.66	3.90	3.25	4.05	2.88	n.d	10.97	0.225
Yb	2.71	3.90	2.52	4.07	3.31	3.80	2.30	1.8	12.00	0.220
Lu	0.45	0.67	0.48	0.68	0.57	0.66	0.40	0.27	2.10	0.0339
$(La/Sm)_N$	0.74	0.96	0.68	0.87	1.05	0.90	2.14	1.65	1.71	1
$(La/Yb)_N$	1.20	1.60	1.08	1.23	1.71	1.68	7.93	9.69	2.57	1

1-2: massive basalts; 3-4: core of pillows; 5: sill; 6: dike I; 7-8: dikes II; 9: keratophyre. $(La/Sm)_N$ and $(La/Yb)_N$: chondrite-normalized ratios. Data analyzed by I.N.A.A at the laboratory of C.N.R.S., Vandoeuvre, France (sample 8 at the geochemical laboratory of the Department of Mineralogy, University of Geneva). Chondrite values are from NAKAMURA (1974).

modern oceanic rocks (cf. MIYASHIRO 1973a; COLEMAN, 1984).

3. Geochemistry

Major and trace element data of the YSPO are listed in table 1, and rare earth element (REE) concentrations in table 2.

As the studied rocks have undergone submarine alteration and greenschist-facies metamorphism, the element immobility has to be discussed. It seems that K, Rb, Sr, and Ba were mobile in all the rocks. Na, Ca, and Al have also strongly migrated in the volcanic rocks, but remained relatively immobile in the well crystallized plutonic rocks. REE, high-field strength elements (HFSE), such as Ti, P, Zr, and Y, and some transition metals, such as Mn, V, Cr, and Ni do not indicate strong migration. This can be partly evidenced by the good preservation of Ap and the limited transformation of primary Ti-Mt into leucoxene and sphene. The good correlation between Ti, P, Zr, Y, V, Cr, and Ni, as well as REE, as shown in the following diagrams, indicates that they behaved in a coherent, immobile fashion. In addition, the close correlation of whole-rock FeO*/MgO ratio with that of their rock-forming Cpx relics (SUN and BERTRAND, 1991), implies that there was no large scale open-type mobilization of these two elements (COISH and CHURCH, 1979; ALABASTER et al., 1982; LAURENT and HEBERT, 1989). Therefore, the observed

whole-rock FeO*/MgO ratios would be those of the primary rocks, and can be used to characterize the degree of the magmatic differentiation for the plutonic and volcanic rocks.

3.1. MAJOR AND TRACE ELEMENTS

The peridotites are homogeneous in chemical composition (Figs 3, 4). Their C.I.P.W. composition corresponds to that of harzburgite and is quite similar to that of the oceanic mantle-peridotites (BONATTI and MICHAEL, 1989) (Fig. 5).

The compositions of the YSPO plutonic rocks are very variable. Their major element variation trends with increasing FeO*/(FeO*+MgO) ratio (where FeO* = FeO + 0.9 Fe_2O_3), from ultramafic cumulates to albitites, are shown in figure 3.

As the element mobilization in plutonic rocks can be impeded by their high crystallinity (SERRI, 1980, 1981), it is likely that the variation tendencies in figure 3 represent the primary nature and reflect the crystallization order throughout the plutonic sequence. These tendencies confirm therefore the crystallization order determined by the petrographic observations: Ol+Cr-Sp; Pl; Cpx; Opx; Ap+Ti-Mt; brown Hbl; zircon; Q. Such variations, in particular, Fe- and Ti-enrichment in the ferrogabbros, indicate a tholeiitic trend, as shown also in A-F-M diagram (Fig. 4). They are comparable to those of high-Ti ophiolite plutonic rocks (SERRI, 1981; SERRI and SAITTA, 1980), particularly to those of ophiolite plutonic rocks from Corsica
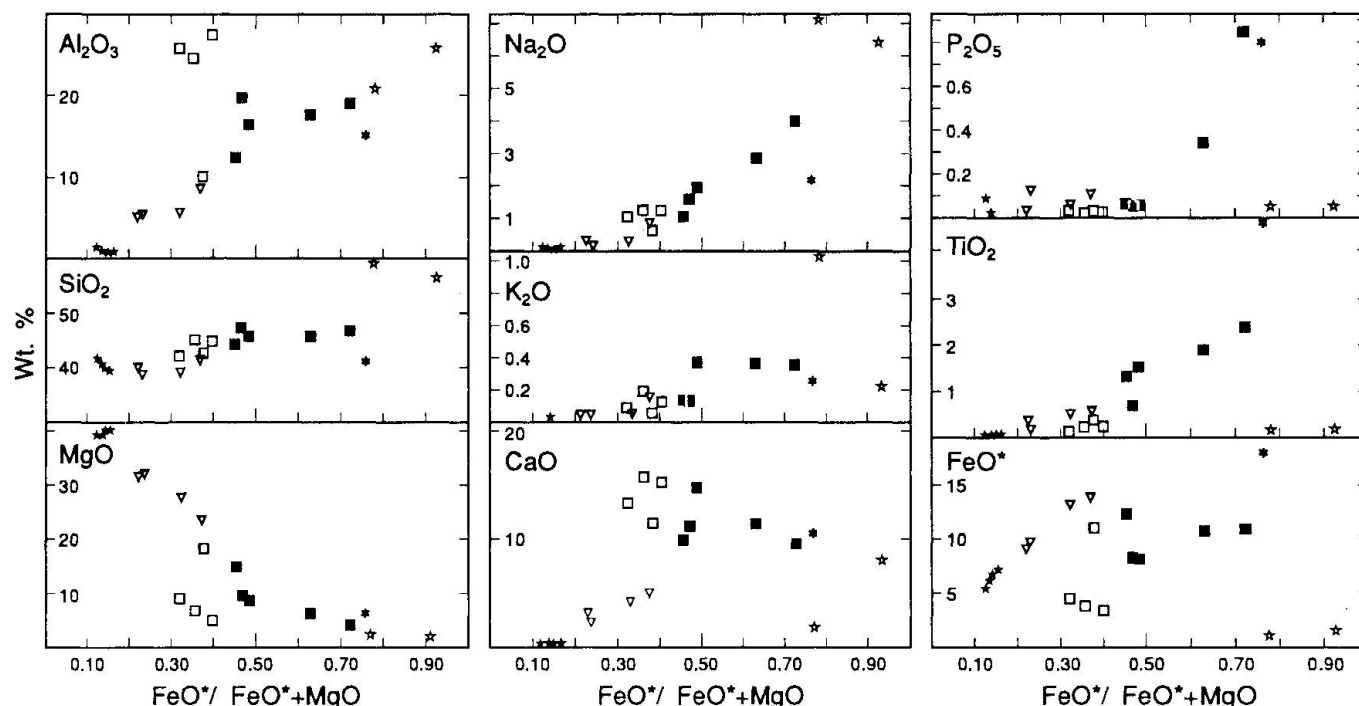
Fig. 3 Major element variation of the YSPO plutonic rocks. Solid stars = mantle-peridotites; inverse open triangles = ultramafic cumulates; open squares = Mg-gabbros (troctolites, Ol-anorthosites and Ol-gabbros); solid squares = gabbronorites; asterisks = ferrogabbros; open stars = albitites.

(OHNENSTETTER and OHNENSTETTER, 1975, 1980), North Apennine (SERRI, 1980) and Western Alps (BERTRAND et al., 1982, 1987), and also to those of the present-day oceanic plutonic rocks (ENGEL and FISCHER, 1975; MIYASHIRO and SHIRO 1981; HEBERT et al., 1983).

For the great majority of the YSPO volcanics, the bulk composition varies from Ol-tholeiite, Q-tholeiite, ferrobasalt to high-Na/low-K intermediate rocks (keratophyre). LILE (large ion lithophile element, such as K, Rb) contents are low in basaltic rocks. However, the dikes II, which have a bulk composition varying from picritic to basaltic, are relatively high in LILE (Tab. 1).

In a A-F-M diagram (Fig. 4), the compositions of the main volcanic rocks are closely analogous to those of modern oceanic rocks (MIYASHIRO and SHIDO, 1980; BYERLY et al., 1976), showing a tholeiitic affinity. The differentiation trend is comparable to that of the high-Ti ophiolites from Corsica (OHNENSTETTER and OHNENSTETTER, 1975), North Apennine (SERRI, 1980), and Western Alps (BERTRAND et al., 1982), and also to that obtained from the experiments of oceanic basalt differentiation at 1 atm and 1 kb (DIXON and RUTHERFORD, 1979, 1982).

As shown before, Ti, P, Zr, Y, V, Mn, Cr, and Ni were immobile during alteration and metamorphism. However, because of the cumulate na-

ture of the plutonic rocks, the concentration of these elements depends not only on the degree of differentiation, but also on the variable amount of liquid situated in the interstices between the cumulus minerals. For this reason, these elements are used mainly for the volcanics in petrogenetic discussions. The relative high content of TiO_2 (> 1.2%) in the great majority of the analyzed volcanic samples clearly indicates an affinity with typical high-Ti Phanerozoic ophiolite volcanics (BEBIEN et al., 1975, 1980, 1987; MARCHAL and OHNENSTETTER, 1984). In discrimination diagrams (Fig. 6) the basalts, sills, and dikes I are concentrated in the fields of ocean-floor basalts (OFB) and mid-ocean ridge basalts (MORB); whereas the dikes II, whose data points are rather scattered, plots mainly in the fields of within-plate basalts (WPB) and plume-type MORB.

3.2. RARE EARTH ELEMENTS (REE)

The massive and pillowed basalts, sills, and dikes I have flat chondrite-normalized REE patterns, which are 10–30 times higher than those of chondrite (Fig. 7). The similarity of REE patterns of these rocks suggests a cogenetic nature. In contrast, the dikes II are characterized by an impor-
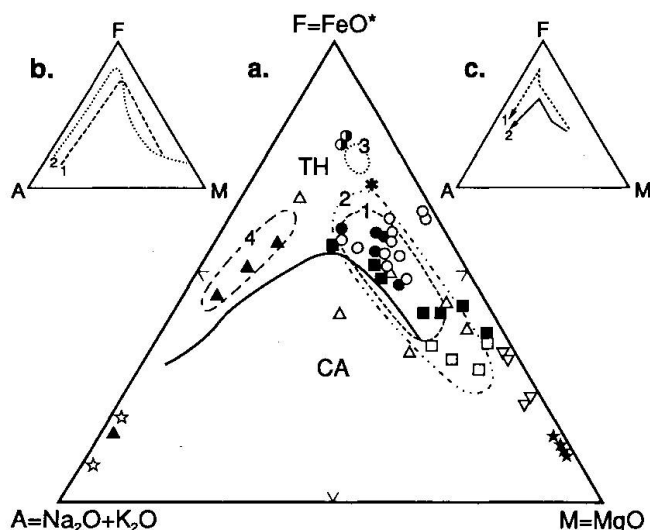
Fig. 4 *(a)* Composition of the YSPO plotted in A-F-M diagram. Field 1 and field 2: abyssal tholeiites and oceanic gabbros, respectively (after MIYASHIRO and SHIDO, 1980). Field 3 and field 4: ferrobasalts and rhyodacites from the Galápagos spreading center (after BYERLY et al., 1976). TH = tholeiitic, CA = calk-alkaline. Open circles = basalts; half-filled circles = ferrobasalts; solid circles = sills and dikes I; open triangles = dikes II; solid triangles = keratophyres; the others symbols as in figure 3. (b) Line 1 and line 2: evolution trend of Corsican ophiolites (after OHNENSTETTER and OHNENSTETTER, 1975) and North Apennine ophiolites (after SERRI, 1980), respectively. (c) Line 1 and line 2: experimentally determined evolution trend of the basalts from the Galápagos spreading center at 1 atm and 1 kb, respectively (after DIXON and RUTHERFORD, 1979, 1982).

Fig. 5 Compositional distribution of mantle-peridotites from different tectonic environments (from BONATTI and MICHAEL, 1989).

tant enrichment of LREE, implying a derivation from another magma type.

In spite of a high REE concentration and a weak LREE enrichment due to a very advanced differentiation, the keratophyres also display a flat distribution pattern similar to that of the basalts, sills, and dikes I. This suggests that the keratophyres represent the differentiated product of the latter.

Consequently, the flat distribution patterns of the plutonic rocks, similar to those of the basalts, sills, and dikes I, would suggest a comagmatic origin for both sequences.

The REE concentrations and the flat normalized distribution patterns of the basalts, sills, and dikes I are closely comparable to those of the ophiolite basalts from North Apennine (BECCALUVA et al., 1980), Corsica (VENTURELLI et al., 1979), and Western Alps (LEWIS and SMEWING, 1980), but different from those of Troodos (KAY and SENECHAL, 1976).

Based on the REE characteristics, SCHILLING et al. (1975) and SUN et al. (1979) divided the
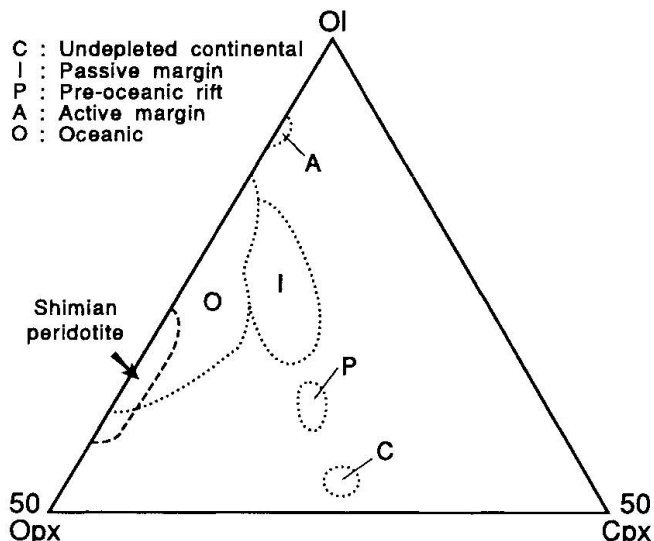
present-day MORB into three types: N-type MORB or LREE-depleted MORB, P-type MORB or enriched-LREE MORB, and T-type MORB or transitional-MORB. On the other hand, BRYAN et al. (1976) pointed out that there are two groups of ocean-floor basalts. The group I, which contains Pl+Ol phenocrysts, is comparable to the N-type MORB; the group II, which contains Cpx phenocrysts, is enriched in LILE and LREE and comparable to the P-type and T-type MORB. These different types can be distinguished in terms of some REE and HSFE ratios (SCHILLING et al., 1975; SUN et al., 1979; LE ROEX et al., 1983, 1985; BRYAN et al., 1976), as summarized in table 3.

The (La/Sm)N, (La/Yb)N, and Zr/Y ratios of the YSPO basalts, sills, and dikes I are low and comparable to those of N-type MORB, or to those of group I basalts defined by BRYAN et al. (1976). Whereas these ratios for the dikes II are very high, corresponding clearly to P-type MORB or Bryan's group II basalts (Tab. 3). This is in agreement with the distinction based on the other trace elements (see Fig. 6) and the phenocryst assemblages (Pl+Ol for basalts, sills, and dikes I, but Cpx for dikes II).

4. Petrogenesis

4.1. PERIDOTITES – STRONGLY DEPLETED MANTLE RESIDUE

In general, MgO in mantle residue increases while CaO and Al_2O_3 decrease with increasing melting
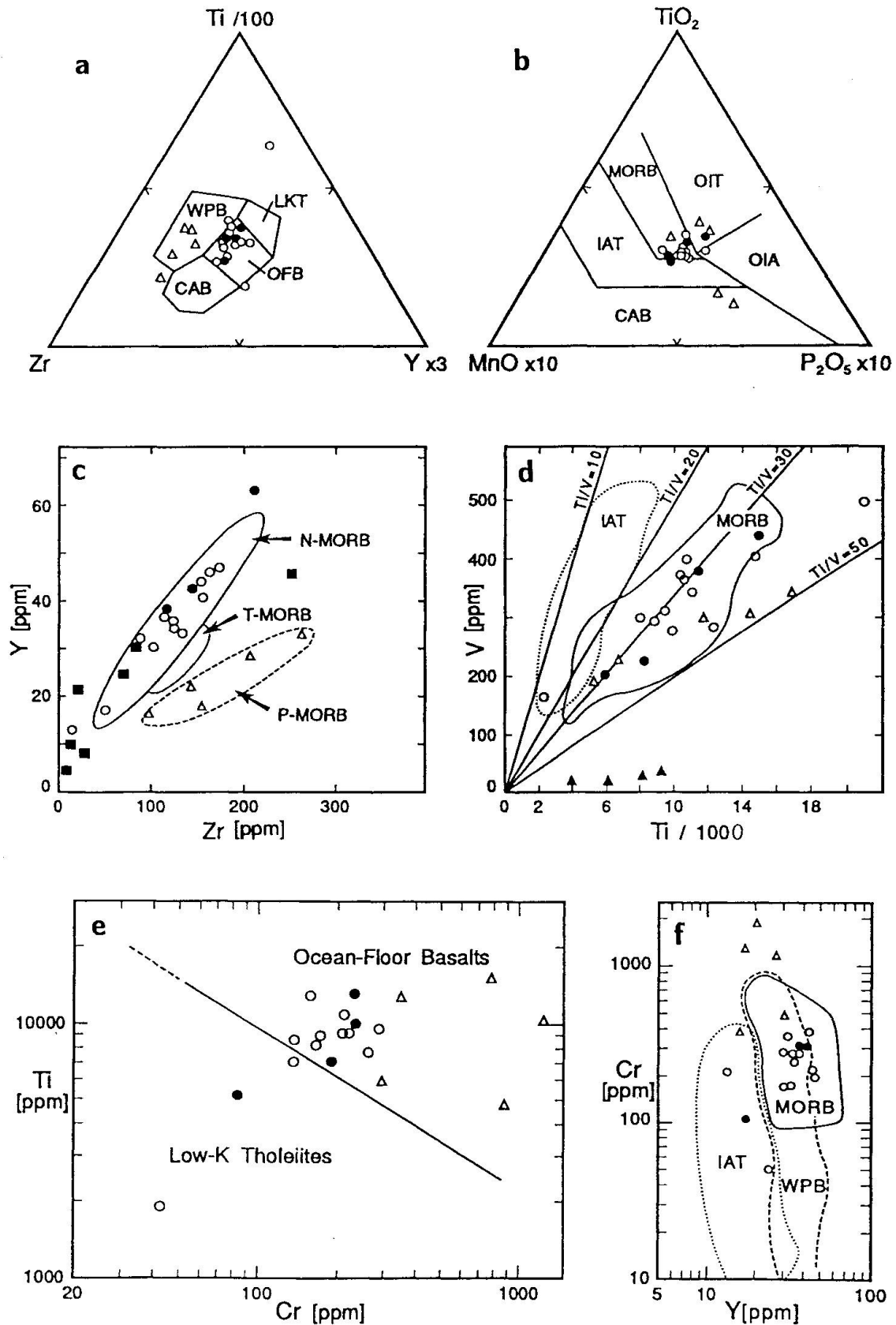
Fig. 6 Plots of trace elements of the YSPO on various discrimination diagrams. (a) After Pearce and Cann (1973), OFB = ocean floor basalts, WPB = within-plate basalts, LKT = low-K tholeiites, CAB = calc-alcali basalts; (b) after Mullen (1983), MORB = mid-ocean ridge basalts, OIT = ocean island tholeiite, IAT = island arc tholeiite, OIA = ocean island alcaline basalts; (c) after the data of basalts from the American-Antartic Ridge (Le Roex et al., 1985); (d) after Shervais (1982); (e) after Pearce (1975); (f) after Pearce(1980). Symbols as in figure 4.

Tab. 3   Some trace element criteria of MORB

Type	(La/Sm)$_N$				(La/Yb)$_N$		Zr/Y	
	a	b	c	d	d	e	b	c
N = I	< 1	0.40–0.70	< 1	0.57–1.03	0.38–1.06	0.35–1.1	2.5	2.2–4.2
T ⎱ II		0.83–1.97	1.1–1.5			1.7–4.3		3.1–4.7
				1–4.09	1.17–13.5			
P ⎰	> 1	1.97	2.4			4.8–6.9		7.1
B.S.DI	0.68–0.90					1.08–1.68		2.43–3.8
DII	1.65–2.14					7.93–9.69		5.94–9

(a) Schilling (1975); (b) Sun et al. (1979); (c) Le Roex et al. (1985); (d) Bryan et al. (1976); (e) Le Roex et al. (1983). N, T, P = normal, transitonal and plume-type MORB. I,II = group I and group II ocean-floor basalts of Bryan et al. (1976). B.S.DI = basalts, sills, and dikes I = suite I; DII = dikes II = suite II.

(Ishiwatari, 1985). The YSPO tectonite peridotites have very high MgO (45-47%, recalculated on the basis of H_2O-free) and very low CaO and Al_2O_3 (< 0.1 and < 1.5%, respectively). This corresponds to a mantle residue after a melting > 30% (Fig. 8a).

As the studied peridotites have been transformed into serpentinites, Ca, Al, and Mg con-

Fig. 7 Chondrite-normalized REE profiles of the YSPO. Normalizing values are from Nakamura (1974). Yt2, Yt6, Yt8 and Yt69 are from Zen (1985) and Lai (1983).

tents must have changed. Therefore, the estimate of degree of partial melting will be more reliable if the composition of primary minerals is considered. The experimental studies on the melting of mantle material (Mysen and Kushiro, 1977; Jaques and Green, 1980) show that Fo content in Ol increases as partial melting progresses. The relict Ol of the tectonite peridotites varies between Fo_{96} and Fo_{97}, which corresponds to a degree of melting between 45 and 70% on the experimental curve (Fig. 8b).

Taking $K_D^{ol-liq} = 0.30$ (Roeder and Emslie, 1970), where $K_D^{ol-liq} = (FeO/MgO)^{olivine}/(FeO/MgO)^{liquid}$, the $[FeO/(FeO+MgO)]^{liquid}$ ratio of the liquid in equilibrium with the relic olivine (Fo_{96-97}) should be within the range of 0.15–0.19. These values are too low to be matched with those of the associated basalts, sills, and dikes I (minimum 0.55), as well as with those of the dikes II (minimum 0.4), so the tectonite peridotites do not represent the residue of the melting event generating the magma of the volcanic rocks.
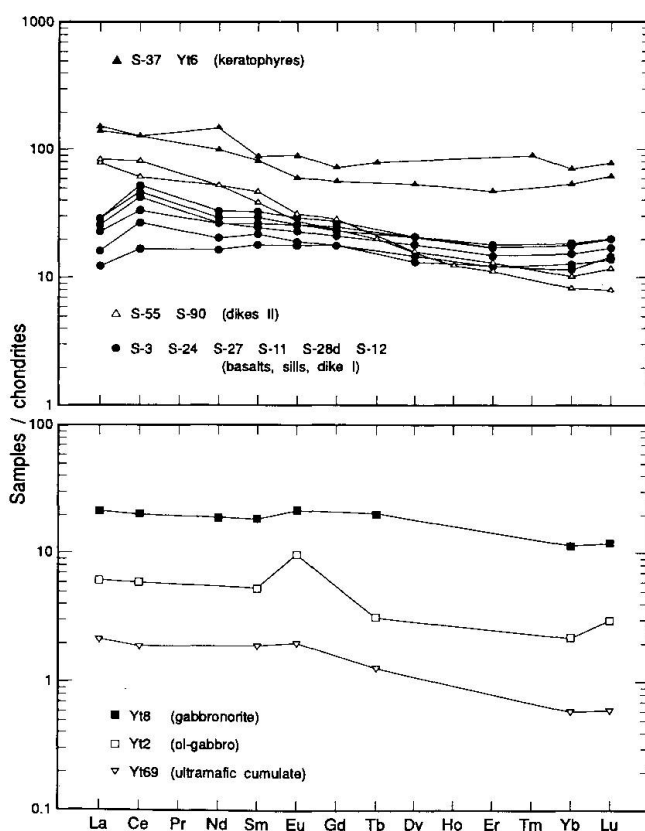
4.2. TWO MAGMATIC SUITES

Using the method of Allegre et al. (1977), the Rayleigh law, which describes the behaviour of trace elements in fractional crystallization process, can be transformed into logarithmic form:

$$\log \frac{C_j}{C_i} = \left[\frac{C°_j}{C°_i} \cdot \frac{D_j-D_i}{D_j-1} \log C°_j \right] + \frac{D_j-D_i}{D_j-1} \log C_j \quad (1)$$

$(D_i > D_j)$

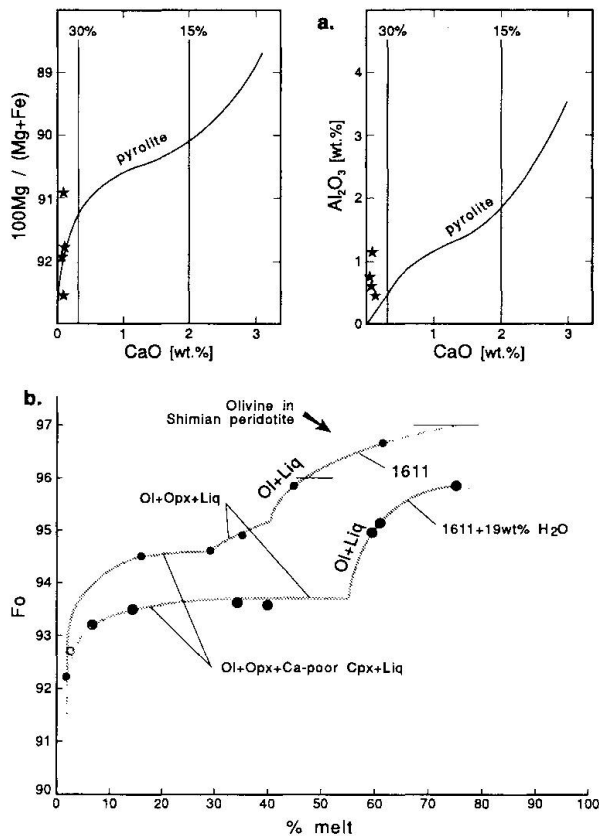C_i, C_j: concentration of trace elements i and j in liquid

Fig. 8 (a) Bulk (simplified after Ishiwatari, 1985) and (b) olivine (after Mysen and Kushiro, 1977) compositional variation of residual mantle-peridotites.
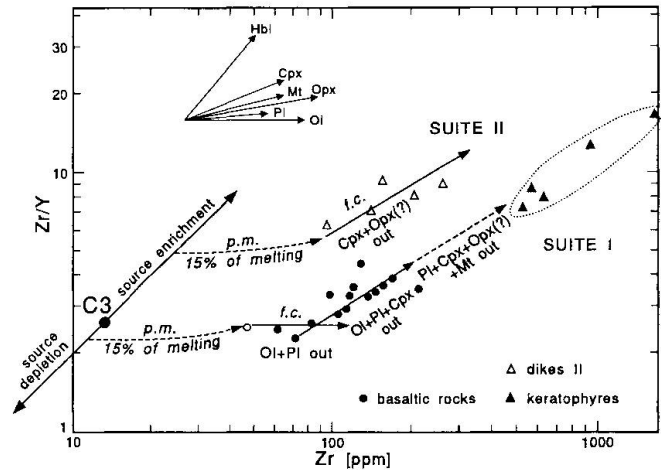

Fig. 9 Zr/Y vs Zr diagram (after Pearce and Norry, 1979; Pearce, 1980; Alabaster et al., 1982) for the YSPO volcanics, showing two magmatic suites and fractionation trends; f.c. = fractional crystallization, p.m. = partial melting.

$C°_i$, $C°_j$: concentration of trace elements i and j in initial liquid

D_i, D_j: bulk distribution coefficient for elements i and j

$Di = \Sigma d_i X_k$

d_i: distribution coefficient for element i between mineral k and liquid

X_k: proportion of mineral k ($0 < k < 1$)

Equation (1) reveals that log (C_j/C_i) is made up of a constant part (first term on the right side of the equation) and a straight-line incremental part (second term on the right side). If the samples belong to a same differential series, at a given C_j value, the C_j/C_i ratio will also be given, that is to say, the composition of the initial magma (represented by the constant part) is defined. By contrast, if the C_j/C_i ratio is considerably different at the same level of C_j value, the constant part should be different. In other words, there are two or more initial magmas.

The petrographic, trace and rare earth element geochemical features described above distinguish two groups of rock types in the YSPO volcanic sequence. The first group includes the basalts, sills, and dikes I, as well as the differentiated ferrobasalts and keratophyres, constituting the great majority of the YSPO volcanic sequence (> 95% vol.%). The second group is represented only by the dikes II.

The differences between the two groups indicate that there are two different magma types, called herein suite I and suite II. This is clearly shown in figure 9 where when Zr = 100, Zr/Y = 3 for suite I and Zr/Y = 6 for suite II.

4.3. PARTIAL MELTING OR FRACTIONAL CRYSTALLIZATION?

Petrographic observation and good correlation between REE concentration show that the suite I volcanic rocks (Fig. 10) are cogenetic. This cogenesis may, however, be explained either by different degree of melting from a same mantle source or by fractional crystallization from a same primary magma.

The distinction between these two processes can be made by plotting the basalt data in the La/Sm vs La diagram (Minster and Allegre, 1978) (Fig. 11). Theoretically, this diagram can be expressed by the following equations, which are transformed from the Rayleigh fractional law and from the partial melting equation (Shaw, 1970, equation 11), in considering La as hygromagmatophile ($D_{La} = 0$):

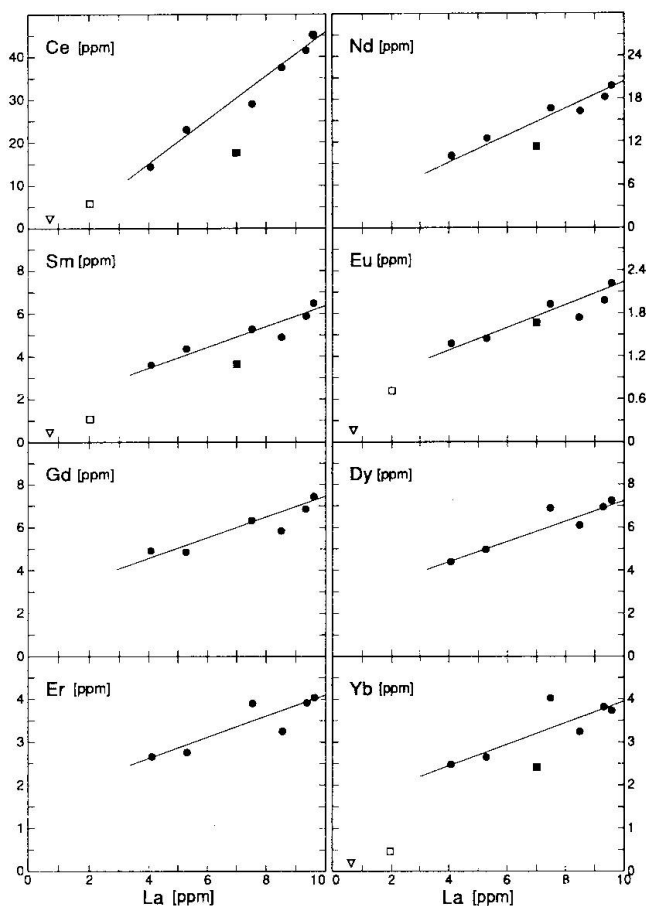$$\frac{La(p)}{Sm(p)} = \frac{La°(p)}{Sm°(p)} [1 - D_{Sm(p)}] + \frac{D_{Sm(p)}}{Sm°(p)} La(p) \quad (2),$$

Fig. 10 REE vs La diagrams of the YSPO suite I volcanics showing cogenetic nature.

Fig. 11 Modelling fractionation curve of the YSPO suite I volcanics (see text) on La/Sm vs La diagram (after ALLEGRE and MINSTER, 1978).

for partial melting (with a designation (p) for each parameter) and

$$\frac{La(f)}{Sm(f)} = \frac{La^\circ(f)^{[1-D_{Sm(p)}]}}{Sm^\circ(f)} \times La(f)^{D_{Sm(f)}} \qquad (3)$$

for fractional crystallization (with a designation (f) for each parameter).

These two equations reveal that: (1) if $La(f)$ > 1 and its variation range is limited (this is always the case for basalts), then in La/Sm vs La diagram, $La(f)/Sm(f)$ appears to be a straight line, like that of $La(p)/Sm(p)$; and (2) the slope of $La(p)/Sm(p)$ is greater than that of $La(f)/Sm(f)$.

The YSPO suite I volcanics ($La = 4.07–9.6$) display a good straight line with a slope of 0.0759 (the deviation of one point is due to accumulation of Pl and Tt) (Fig. 11). Although this sub-horizontal line is not parallel to the horizontal fractionation line defined by ALLEGRE and MINSTER (1978), it is parallel to the fractionation trend of the Reykjanes Ridge basalts. Obviously, the horizontal fractional line corresponds to the Ol- and Pl-frac-
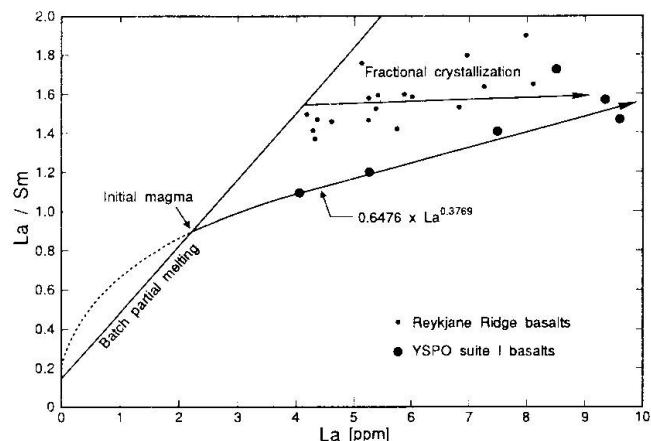
tionation because the DSm for both minerals are close to zero [see equation (2)]. The sub-horizontal line suggests that the compositional variation of the suite I volcanics is controlled by fractionation and that the Cpx-crystallization has taken part in the magmatic evolution.

Using the method of ALLEGRE et al. (1977), $D_{Sm(f)}$ is calculated to be 0.3769 for suite I. Therefore, the variation of La/Sm vs La (Fig. 11) can be expressed as follows:

$$La/Sm = 0.6476 \times La^{0.3769}$$

The extrapolated intercept with the partial melting line may be the "initial" magma composition for the suite I volcanics if $D_{Sm(f)}$ always remains the same, but the curve on the left side of this intercept is not realistic.

4.4. NATURE OF THE MANTLE SOURCE

As shown above, the variation of the chondrite-normalized $(La/Sm)_N$ and $(La/Yb)_N$ ratios in each suite (Tab. 3) is controlled by fractional crystallization. Obviously, the composition of the most La-depleted sample may be nearer to that of the "initial" magma derived by partial melting from the mantle (Fig. 11). Such ratios can therefore indicate some characteristics of the mantle source.

Note that the absolute REE concentrations in the "primitive mantle" (SUN, 1982; HOFMANN, 1988) are higher than those of the chondrite, but their Sm/La and Yb/La ratios are very similar. So the chondrite-normalized $(La/Sm)_N$ and $(La/Yb)_N$ ratios in table 3 are the same as those normalized on the primitive mantle, the most probable can-

didate for the mantle source of basaltic rocks (ibid).

The main minerals in the mantle are Ol, Opx, and Cpx, as well as minor amount of Sp, Gar, and Pl, depending on pressure. Experimental studies on peridotite melting (JAQUES and GREEN, 1980) demonstrated that the stability ranges for Pl, Sp, and Gar are < 10 kb, 10–20 kb, and > 20 kb, respectively. The magmas derived from the Pl-peridotite, Sp-peridotite, and Gar-peridotite are of composition of Q-tholeiite, Ol-tholeiite, and alkaline picrite, respectively (ibid). The less evolved YSPO suite I volcanics are of Ol-tholeiite composition, suggesting that their mantle source is of Sp-peridotite composition.

Although the published absolute D values are variable, the order $D_{La} < D_{Sm} < D_{Yb}$ remains for all the mantle minerals except Pl (cf. WOOD, 1978, his Tab. 12; MINSTER and ALLEGRE, 1978, their Tab. 1).

In order to examine the variations of the $(La/Sm)_N$ and $(La/Yb)_N$ ratios of the liquid during low degree equilibrium melting, we transform equation from SHAW (1970) as follows:

$$\left(\frac{C_j}{C_i}\right) N = \left(\frac{C^\circ_j}{C^\circ_i}\right) N \frac{D_i + F(1-D_i)}{D_j + F(1-D_j)} \qquad (4)$$

Where i = Sm or Yb; j = La; F = fraction of liquid (0 < F < 1)

If the partial melting takes place directly in the primitive mantle, that is, $(La^\circ/Sm^\circ)_N = 1$, then the $(La^\circ/Sm^\circ)_N$ ratio should be > 1 since $D_{La} < D_{Sm}$. The fact that $(La/Sm)_N < 1$ for the suite I volcanics (Tab. 3) precludes any possibility of a direct partial melting from the primitive mantle.

Therefore, it is necessary that the mantle source for the suite I volcanics should be depleted. The primitive mantle should have been depleted at least one time (melting 1) before it was remelted (melting 2) for yielding the magma of the suite I. Thus, in replacing the $(C^\circ_j/C^\circ_i)_N$ by the composition of the residual solid derived from the melting 1, the two-stage melting process can be expressed by the following equation (the subscripts 1 and 2 with each parameter refer to melting 1 and 2, respectively):

$$\left(\frac{C_j}{C_i}\right) N = \left(\frac{D_{j1}}{D_{i1}}\right) \frac{D_{i1} + F_1(1-D_{i1})}{D_{j1} + F_1(1-D_{j1})} \times \frac{D_{i2} + F_2(1-D_{i2})}{D_{j2} + F_2(1-D_{j2})} \qquad (5)$$

In the simplest case, for example, low degree melting for both stages during which the mineral proportions remain invariable (i.e. $D_{j1}/D_{i1} = D_{j2}/D_{i2} = $ constant), if the degree of the melting 2 is known (determined by another method), the estimate of the nature of the mantle source is possible.

Assuming that the mantle mineral assemblage for the volcanics is Ol + Sp = 0.6 ($D^{ol} = D^{Sp}$), Cpx = 0.2, and Opx = 0.2, we can calculate the bulk distribution coefficients (using the data of FREY et al., 1978, set 1 in their Tab. A-1), which are:

$$D_{La} = 0.01, \ D_{Sm} = 0.03, \ D_{Yb} = 0.1$$

The least evolved suite I basalt sample has $(La/Sm)_N = 0.68$ and represents the magma derived from a melting of about 15% (see Fig. 9). When F2 = 0.15, $(La/Sm)'_{N2} = 1.1$ (corresponding to the value of direct melting from primitive mantle), so $(La^\circ/Sm^\circ)_{N2} = 0.62$, corresponding to a depleted mantle source after 1.3% ($F_1 = 0.013$) of melting 1 from the primitive mantle (Fig. 12). In the same way, we can construct the same graphic as in figure 12 for the $(La/Yb)_N$ ratio. With $(La/Yb)_N = 1.08$ and $F_2 = 0.15$, we can estimate $(La^\circ/Yb^\circ)_N = 0.72$, corresponding to $F_1 = 0.0043$.

For the YSPO suite II volcanics, $(La/Sm)_N > 1$ (minimum 1.65), this can be explained by a low degree of melting (F < 0.015) directly from the primitive mantle, or from an already enriched mantle. The latter source seems to be more likely, because F_2 is evaluated to be about 0.15 (Fig. 9); at this level, $(La/Sm)'_{N2} = 1.1$. This requires a mantle source of which $(La^\circ/Sm^\circ)_{N2}$ should be greater than 1 (1.65/1.1 > 1), that is to say, an enriched mantle (Fig. 12). This consideration is in agreement with the graphic estimate based on the Zr/Y vs Zr variation (Fig. 9), proposed by PEARCE and NORRY (1979), PEARCE (1980), and ALABASTER et al. (1982).

4.5. FRACTIONAL CRYSTALLIZATION ORDER

The order of mineral accumulation in the plutonic sequence is already determined by petrographic observations and confirmed by major element variations (Fig. 3). With regard to the volcanic rocks, this order can be ascertained by the association of phenocrysts and by the regular variations of some trace elements.

For the suite I volcanics, several samples of basalts, in particular pillow lavas, contain Pl and Ol phenocrysts in Cpx-bearing matrix, suggesting that Pl crystallized before Cpx. This suggestion is confirmed by the variation trend in Zr/Y vs Zr diagram (Fig. 9), where the trend firstly follows Ol and Pl fractionation vectors, then Cpx and Opx vectors. Although Cr-Sp phenocrysts have not been found in these rocks, the decrease of Cr (D_{Cr} > 1) with increasing Y (D_Y < 1) contents (Fig. 6f) indicates the existence of such a fractionation.

The ferrobasalts may be considered to represent a product extremely enriched in Fe and P
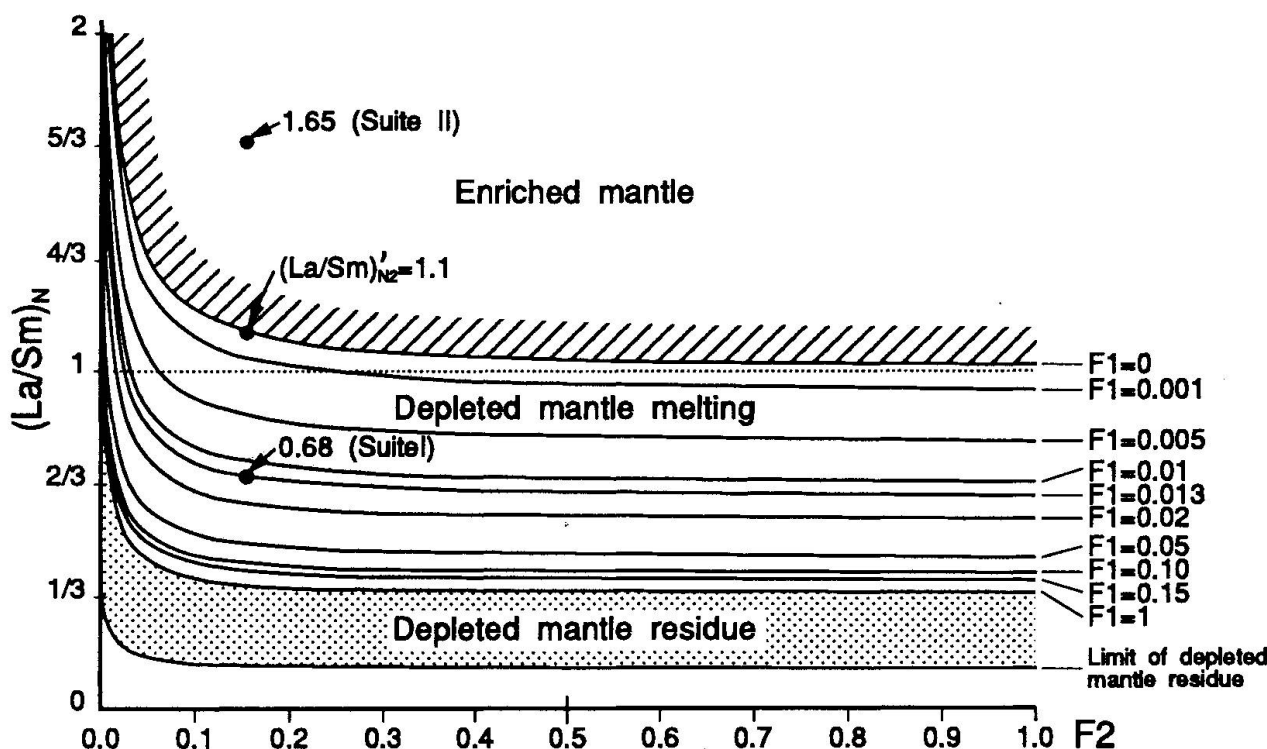
Fig. 12   Normalized $(La/Sm)_N$ variation in two-stage melting (F1 and F2) process [based on equation (5), see text].

resulting from the fractional crystallization of Ol and Pl, followed by Cpx and Opx for the suite I volcanics. The keratophyres show the greatest enrichment in SiO_2 and Na_2O, as well as in incompatible elements such as Zr, Y, and Hf, and the greatest depletion in compatible elements such as Mg, Cr, and Ni. They can be regarded as the ultimate product of Ol+Pl+Cpx+Opx fractionation, followed by Ti-Mt crystallization for suite I volcanics (Figs 6d, 9). The remarkable gap of Ti, V, Zr, Y, and Cr concentrations between basaltic rocks and keratophyres (Tab. 1) implies that the Ti-Mt fractional crystallization was important.

Therefore, the fractional crystallization order for the suite I volcanics is the following: Cr-Sp+Ol; Pl; Cpx; Opx; Ti-Mt, similar to that of the plutonic sequence. Such an order is comparable to that of MORB from the East Pacific (PEARCE et al., 1986). The appearance of Cpx phenocrysts in the suite II rocks indicates that Cpx crystallized prior to Pl. This can also be shown in figure 9 where their trend follows the Cpx and Opx vectors. The similarity of crystallization order of liquidus minerals between the plutonic sequence and the suite I volcanics enhances therefore their comagmatic nature, as proposed above on the basis of comparison in normalized REE distribution patterns. This comagmatism is also supported by the similar chemical features of the primary Cpx from the two sequences (SUN and BERTRAND, 1991).

4.6. MAGMATIC EVOLUTION

As demonstrated in the petrography part, the main silicate minerals constituting the YSPO are represented by the four phases: Ol, Pl, Cpx, and Opx. Thus, the different rock types can be considered as being determined by varying proportions of these minerals in a four-component Ol-Pl-Di-Q system. Experiments on basaltic magma show that, as pressure increases, the Pl crystallization field contracts while the Cpx field expands (BENDER et al., 1978; PRESNALL et al., 1978, 1979) (Fig. 13a).

The crystallization of Ol, and particularly of Pl, prior to Cpx in both plutonic and suite I volcanic rocks suggests that the fractional crystallization in the magma of these two sequences was performed at low pressure, probably less than 5 kb (PRESNALL et al., 1978, 1979). In contrast, the crystallization of Cpx prior to Pl in the suite II volcanics indicates a relatively high pressure (> 5 kb).

As there is no great change in phase relationship at low pressure (1 atm to 5 kb, Fig. 13a), the ranges of formation and the "liquid line of descent" paths for the plutonic and suite I volcanic rocks can be illustrated by a 1-atm pseudo-quaternary Ol-Pl-Di-Q diagram (Fig. 13b). It should be mentioned that pigeonite has not been observed in the YSPO, therefore the crystallization field of
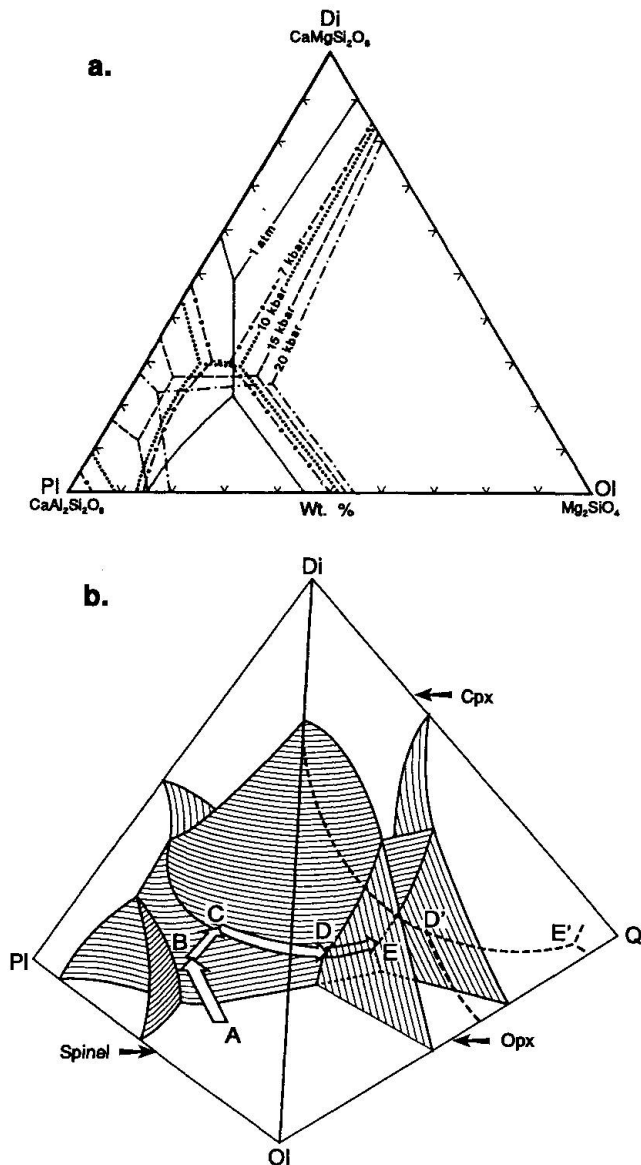
Fig. 13 (a) Ol-Pl-Di phase diagram showing an expansion of Cpx crystallization field with increasing pressures (PRESNALL et al.. 1978, 1979). (b) Basaltic magma evolution in the 1-atm Ol-Pl-Di-Q system (simplified after PRESNALL et al., 1979, CHRISTIE and SIN TON, 1986), projection onto the Ol-Di-Q face is after WALKER et al., 1979). It is likely that the ultramafic cumulates, troctolites, Ol-gabbros, gabbronorites and ferrogabbros crystallized in Ol-volume (A → B), Ol-Pl cotectic surface (B → C), Ol-Pl-Cpx cotectic curve (C → D), Ol-Pl-Cpx-Opx reaction point (D), and Pl-Cpx-Opx cotectic curve (D → E), respectively.

this mineral was omitted in figure 13b. Such a simplification has also been used by some other authors (WALKER et al., 1979; STOLPER, 1980).

It can been seen that the ultramafic cumulates should have crystallized in the Ol-volume (A → B), the troctolites and the Ol-anorthosites on the Ol-Pl cotectic surface (B → C), and the Ol-gab-

bros along the Ol-Pl-Cpx cotectic curve, the gabbronorites at the (C → D). It is interesting to note that the ultramafic cumulates and the Mg-gabbros sometimes show alternating Ol-rich and Pl-rich layers, this implies that some new "primary" magma would have been added to the evolved magma (B → C) in driving the latter back again to the Ol-volume.

The gabbronorites, in which Hyp (hypersthene) occurs as intercumulus, could have been formed at the Ol-Pl-Cpx-Opx reaction point. This reaction can be demonstrated by the following textures: (1) Ol is rimmed by Opx coronas; (2) Ol (altered), Pl, and corroded Cpx are included in large crystals of Hyp. The liquid composition cannot move away from the point D until the Ol in contact with the liquid is exhausted. The ferrogabbros, in which the Hyp appears as cumulus phase, should have been formed along the Pl-Cpx-Opx univariant curve (D → E). The important appearance of Ap (apatite), Ti-Mt, and brown Hbl in the ferrogabbros suggests that the magma lying on the Pl-Cpx-Opx curve (D → E) was enriched in P, Fe, and Ti, and that water pressure (P_{H_2O}) and oxygen fugacity (fo_2) were also relatively high. In addition, the rarity of ferrogabbros suggests that the amount of liquid saturated in Ti-Mt have been very limited. The albitites, which are rarer and appear only in veins, might represent the ultimate residual liquid lying on the D → E curve, probably approaching the eutectic point E.

The geochemical study of the Cpx from the Yanbian plutonic sequence (SUN and BERTRAND, 1991) showed that, as Fe/Mg and Ti of bulk composition increase from ultramafic cumulates to ferrogabbros, Fe/Mg of the primary Cpx increases simultaneously; Ti in the Cpx, however, which increases from ultramafics to Mg-gabbros and culminates in the gabbronorites, abruptly decreases in the most Ti-rich ferrogabbros. This phenomenon is also observed in the typical Phanerozoic high-Ti ophiolite cumulates, such as the Rocciavré ophiolites in the Alps (POGNANTE et al., 1982). With the 1-atm pseudo-quaternary Ol-Pl-Di-Q system, this particularity can be readily explained. Since the gabbronorites crystallized from the liquid situated at the Ol-Pl-Cpx-Opx reaction point, where a dramatic increase in Fe and Ti and a mild decrease in Si (SiO_2-undersaturated) occurs in the liquid (GROVE and BAKER, 1984), Ti can easily enter the Cpx structure following the substitution formula $Ti^{vi} + (0.4\ Al^{vi} + 1.6\ Al^{iv}) = 2.6 - (M^{vi} + 1.6\ Si^{iv})$ (M = bivalent cation) (SUN and BERTRAND, 1991). Therefore, the high-Ti Cpx can be formed in the gabbronorites. However, as the ferrogabbros crystallized from the liquid lying on
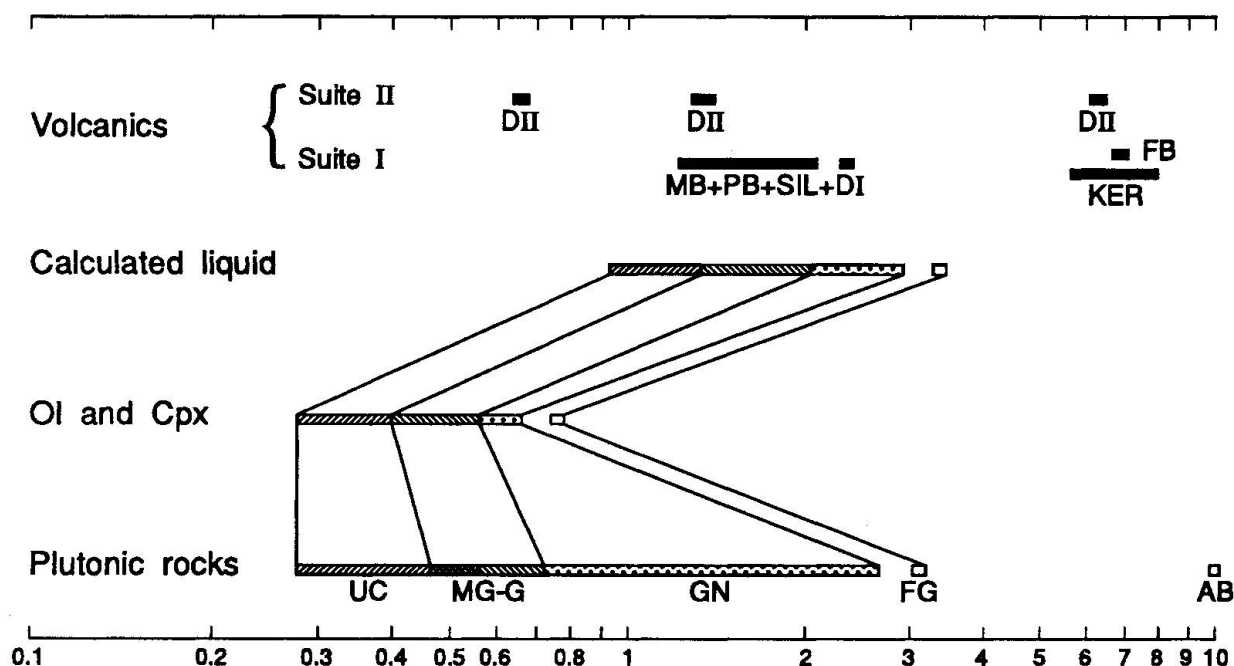
Fig. 14 Magmatic correspondence between plutonic and suite I volcanic rocks in terms of FeO*/MgO ratios. Abbreviations as in table 1.

the Pl-Cpx-Opx curve, which is not only enriched in Fe and Ti, but also in SiO_2, according to the above substitution formula, the SiO_2-saturation would prevent Ti in the liquid from entering the Cpx structure. Thus, the Cpx are depleted in Ti. As GROVE and BAKER (1984) pointed out, when the liquid leaves the Ol-Pl-Cpx-Opx reaction point, the SiO_2-increase could trigger Mt-saturation, this accounts for the abundant Ti-Mt in the ferrogabbros and the gap of some incompatible element concentrations (Ti, V, Zr, Y) between basaltic rocks and keratophyres (Figs 6d, 9).

4.7. MAGMATIC CORRESPONDENCE BETWEEN PLUTONIC AND VOLCANIC ROCKS

The YSPO volcanics are aphyric and porphyritic; in the latter, the amount of phenocrysts is quite low (< 5 vol.%). Hence, these rocks may be regarded as representing the liquid. Since the plutonic and suite I volcanic rocks are comagmatic, as demonstrated before, there should be some original magmatic relationship between the two sequences.

This correspondence can be found by plotting the volcanic compositions onto some sections in the Ol-Pl-Di-Q system, as has been done in the investigations of modern oceanic basalt evolution by several authors (WALKER et al., 1979; STOLPER, 1980; GROVE and BRYAN, 1983; CHRISTIE and SINTON, 1986). If the volcanics are not altered, then

their compositions lie on or near the phase boundary curves concerned. The great majority of the MORB are located on the Ol-Pl-Cpx curve, some evolved ferrobasalts lie near to the Ol-Pl-Cpx-Opx reaction point, and the rhyodacites at the Pl-Cpx-Opx curve approaching to the Q apex (GROVE and BAKER, 1984; BRYAN, 1983; WALKER et al., 1979).

As the FeO*/MgO ratio of the magma varies continuously with the magmatic evolution, it has been used to indicate the degree of magmatic differentiation in the investigation of volcanic rocks (MIYASHIRO, 1973b, 1974, 1975). Since there is an equilibrium of this ratio between the minerals and the magma from which they crystallized, the correspondence between plutonic rocks and associated volcanic rocks can be defined by comparing the FeO*/MgO ratios of cumulus Ol, Cpx, and Opx in plutonic rocks with those of the same mineral phenocrysts in volcanic rocks. Unfortunately, as in the majority of the ophiolites, the Ol phenocrysts in the YSPO are completely altered, and the Cpx and Opx phenocrysts do not occur in the suite I volcanics. Therefore, such a comparison is not possible. Nevertheless, as the compositions of cumulus minerals in the plutonics have been analyzed, the FeO*/MgO ratios of the magma in equilibrium can be calculated with the distribution coefficient (KD). Thus, in comparing the calculated FeO*/MgO ratios of the plutonic-forming magma with those of the observed volcanics, the correspondence can also be established.

ROEDER and EMSLIE (1970) determined in the laboratory that the distribution coefficient K_D^{ol-liq} is about 0.30. They pointed out that, between 1150 and 1300 °C, this coefficient is independent of temperature. Later, BENDER et al. (1978) specified that this value may slightly increase with decreasing temperature and increasing pressure. Since the MORB magmatic fractionation usually takes place in this temperature interval (1150–1300 °C), the value of $K_D^{ol-liq} = 0.30$ is consistent with that determined from Ol phenocrysts in the abyssal tholeiites (HEKINIAN et al., 1976; MIYASHIRO and SHIDO, 1980). Therefore, this value has been accepted and widely used in the investigation of oceanic and ophiolitic rocks (CHURCH and RICCIO, 1977; MIYASHIRO and SHIDO, 1980; PRESNALL et al., 1979; SERRI, 1980, 1981; BECCALUVA et al., 1980). With respect to the distribution coefficient $K_D^{cpx-liq}$, values seem to be more variable. 1-atm experiments on primitive basalts from the *FAMOUS* area on the Mid-Atlantic Ridge gave a value of 0.23 (GROVE and BRYAN, 1983). But on the other hand, in 1-atm experiments on an alkaline basalt from Lihir Island (Papua New Guinea), this value is 0.21 (KENNEDY et al., 1990). In addition, the values such as 0.25 (GROVE and BAKER, 1984), 0.236 (CHURCH and RICCIO, 1977) and 0.26–0.27 (SERRI, 1980) have also been estimated and used in the interpretation of magmatic fractionation. The reason for the variations of this distribution coefficient values is not yet well known. In the YSPO Ol-gabbros, both Ol and Cpx are cumuli, suggesting that these two minerals were in equilibrium with their parental liquid when they crystallized. Thus, if the compositions of the two coexisting minerals are known and the K_D^{ol-liq} is given, then the $K_D^{cpx-liq}$ can be readily calculated as follows:

$$K_D^{cpx-liq} = [(FeO/MgO)^{cpx}/(FeO/MgO)^{ol}] K_D^{ol-liq}$$

In the Ol-gabbros, the FeO*/MgO ratios of Ol and Cpx are 0.491 and 0.441, respectively, so the calculated $K_D^{cpx-liq}$ is 0.27. This value is comparable to that estimated by SERRI (1980) for the plutonic rocks of the Apennine ophiolites. The calculated FeO*/MgO ratios of the liquid in equilibrium with the plutonic rocks are: 0.93–1.35 for ultramafic cumulates, 1.33–2.15 for Mg-gabbros, 2.15–2.43 for gabbronorites, and > 2.43 for ferrogabbros (Fig. 14).

The FeO*/MgO ratios for the great majority of suite I basaltic rocks vary within the range of 1.22–2.14 (two Tt-rich samples have values of 2.44 and 2.82). Compared to the calculated FeO*/MgO ratios of the liquid from which the plutonic rocks crystallized, these basalts correspond mainly to the liquid for the Mg-gabbros (FeO*/MgO =

1.33–2.15), and for a small part, to the liquid for the ultramafic cumulates. The two Tt-rich samples might correspond to the liquid for the gabbronorites. The ferrobasalt samples, which have FeO*/MgO ratios as high as 6.80–6.99, might correspond to the liquid for the ferrogabbros. The keratophyres, having very high FeO*/MgO ratios (5.46–8.14), could represent the most evolved residual liquid.

5. Geotectonic environment

It is generally accepted that ophiolites represent the remnants of oceanic crust generated in different environments: mid-ocean ridges, fore-arc basins, back-arc basins (marginal basins), immature island-arcs, incipient oceanic basins, and "leaky" transform faults (COLEMAN, 1977, 1984; SERRI, 1981; PEARCE et al., 1984).

The immature island-arc, fore-arc basins, and back-arc basins formed in a supra-subduction zone (SSZ). The great majority of the most studied SSZ ophiolites, such as those of the Eastern Mediterranean, display both MORB and IAT (island-arc tholeiite) affinities (PEARCE et al., 1984). Some SSZ ophiolites, such as those of the Bay of Islands (ELTHON, 1991) and East Taiwan (JAHN, 1986), are very similar to MORB in the conventional chemical discrimination diagrams.

Due to Sr-mobility during metamorphism and insufficient accuracy for Nb and Y (analyzed by XRF), the YSPO volcanics plot in the field overlapped by N-MORB, E-MORB, and BABB (back-arc basin basalts) in the recently established $Ce_N-Sr_N-Sm_N$ (IKEDA, 1990) and La/Nb vs Y (FLOYD et al., 1991) diagrams. Therefore, the "key elements" for discrimination of tectonic environments should be Th and Ta (PEARCE, 1991), but at present, no data are available for the YSPO.

The overall petrographic (Pl prior to Cpx) and geochemical data (MORB) do not show any IAT signature for the YSPO (Figs 3, 4, 6). Moreover, in the Yanbian-Shimian zone, there is no contemporaneous arc-related volcanism, but pre-ophiolite continental rifting volcanism. This suggests that, at least for the moment, the SSZ origin is not likely for the YSPO.

The formation of incipient oceanic basins is generated by separation of continental crust resulting from rifting (COLEMAN, 1984). Whether the expansion rate is fast (Gulf of California) or slow (Red Sea), the compositions of the basalts erupted from the spreading centers in these basins are very similar to typical MORB (cf. ALTHERR et al. [1988] for the basalts from the Red See, and SAUNDERS et al. [1982] for the basalts from the

Gulf of California). It is therefore difficult to distinguish between them if only the geochemical data are used. Nevertheless, the spatial distribution of these basalts and associated non-MORB rocks can provide useful informations (COLEMAN, 1984). In the Red Sea area, MORB occurs in the axial spreading trough, whereas the dikes, stratified gabbros, and bimodal volcanics (basalts vs rhyolites and granites) are developed in the margins of the separated continents (COLEMAN and McGUIRE, 1988). As the Gulf of California is near to the continent, the sedimentary rate is extremely high. Thus at the northern end of the Gulf (Guaymas Basin), the erupted magma does not reach the basin surface to form flows, but occurs as sills intercalated within the sediments (SAUNDERS et al., 1982). Far away from the continent, for example, at the connexion with the East Pacific Rise, the basalts occur mainly as flows (predominant massive basalts with some pillow lavas); sills are much less abundant (ibid.).

In the YSPO volcanic sequence, three particularities must be emphasized: (1) very advanced differentiation for the suite I magma, (2) coexistence of dominant N-MORB (suite I) with minor P-MORB (suite II), and (3) sills, massive basalts, and sediments concentrated in the lower part of the volcanic pile whereas pillows predominate in the upper part. The ferrobasalts are quite common in oceanic environments, such as in the Galápagos spreading center (CLAGUE and BUNCH, 1976; CLAGUE et al., 1981; BYERLY et al., 1976; BYERLY, 1980), East Pacific Rise (CAMPSIE et al., 1984; PEARCE et al., 1986), Juan de Fuca Ridge (CLAGUE and BUNCH, 1976), South-West Indian Ridge (LE ROEX et al., 1983), Mid-Atlantic Ridge (BRYAN et al., 1988). However, the association of basalts-ferrobasalts-keratophyres appears more restricted, it has been observed at the Galápagos spreading center (basalts-ferrobasalts-andesites-rhyodacites-rhyolites) (BYERLY et al., 1976; CLAGUE et al., 1981), East Pacific Rise (CAMPSIE et al., 1984), and Iceland rift zone (IMSLAND, 1983). On the other hand, the coexistence of N-MORB with minor P-MORB has also been observed at hot-spot-influenced oceanic localities, such as the Galápagos spreading center (BYERLY et al., 1976; SCHILLING et al., 1982), American-Antarctic Ridge (LE ROEX et al., 1985), East Pacific Rise (4–20.5°) (CAMPSIE et al., 1984), and some segments on the Atlantic Ridge (7°S, 54°S, 45°S) (BRYAN et al., 1976). It should be noted that most of the localities mentioned above are situated at or near transform faults. The magmas derived from such environments are more fractionated than those from normal mid-ocean ridges (HEKINIAN and THOMPSON, 1976).

Comparing with the characteristics of present-day oceanic environments, it is likely that the YSPO were formed at hot-spot-influenced spreading centers in the vicinity of transform faults or directly in the latter. The appearance of abundant sills and sediments in the lower part of the YSPO volcanic sequence implies that the basins in which the basalts erupted and sediments were deposited could have been near to the continent, that is to say, small incipient oceanic basin(s). Towards the upper part of the volcanic pile, both sills and sediments become relatively rare, suggesting that the spreading center(s) might have been more distant from the continent. In addition, the fact that sheet-flows (massive basalts) dominate in the basal part, and pillows dominate in the upper part of the volcanic sequence implies at least two eruption episodes. As demonstrated in the investigations on the basalts from the Galápagos spreading center (BALLARD et al., 1979) and the East Pacific Rise (BYERS et al., 1986), the sheet-flows represent early, brief but voluminous eruptions from fast-spreading center(s) on the bottom of a broad rift valley, which were followed by later, sustained, slower but steadier eruptions from slow-spreading center(s) on the bottom of a deep rift valley with rugged relief. It seems likely that these eruption conditions were applicable to the YSPO volcanics.

The formation of small incipient oceanic basin(s) for the YSPO might result from rifting on the Archean to Early Proterozoic continent (crystalline foundation). This process is evidenced by an early bimodal magmatism in the Shimian-Yanbian region. For example, in the eastern zone, the bimodal volcanism is demonstrated by the development of alkaline basalts on one hand, and rhyolites and tranchyandesites on the other hand, with 1605 ± 27 Ma (Rb–Sr) for the alkaline basaltic tuffs, 1685 Ma and 1676 Ma (U–Pb, zircon) for the tranchyandesites, and 1685 Ma (K–Ar) for the diabase dikes (CHEN and WANG, 1987; LUO, 1983, 1988; YUAN et al., 1985). This bimodal magmatism is also demonstrated by intrusions of stratified gabbros and syenites in the crystalline basement. An example is the Panzhihua complex, which has an age as early as 1508 ± 5 Ma ($^{40}Ar–^{39}Ar$, analyzed on Cpx of gabbros, YANG and JIANG, 1988). Therefore, the continental rifting might be responsible for the break-up of the ancient continent (Archean to Early Proterozoic) and the formation of the small oceanic basin(s) in which the YSPO developed later.

It is important to note that along the Shimian-Yanbian zone, several outcrops of mafic-ultramafic complexes have been found (Fig. 1). Although
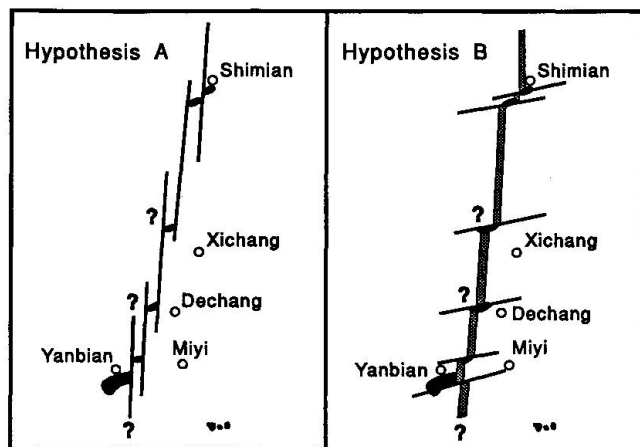
Fig. 15   Two alternative geotectonic environments for the YSPO.

little study has been done until now, these complexes would probably be the same type of ophiolites as the YSPO.

In view of the arguments presented here, it seems very likely that ophiolites in the Shimian-Yanbian Proterozoic orogenic belt were formed in small incipient oceanic basin(s), generated by the separation of an ancient continent (Archean to Early Proterozoic crystalline foundation). The possible original location of the YSPO might be either in a hot-spot-influenced ridge intersected by long transform faults or in the latter. Naturally, the present emplacement of these ophiolites does not represent their original position, but if the tectonic displacement distance is neglected, as has been done by many ophiolite-researchers, the distribution of the ophiolites in the Shimian-Yanbian belt can be shown by the following two alternative hypotheses (Fig. 15):

(1) the ophiolites were formed in a ENE–WSW spreading ridge, cut by long NNE–SSW transform faults;

(2) the ophiolites were located in ENE–WSW transform faults, which cut the NNE–SSW spreading ridge.

6. Conclusions

The petrographic and geochemical data of the YSPO plutonic and volcanic sequences are closely comparable to those of typical Phanerozoic high-Ti ophiolites, particularly the North Apennine and the Western Alps, and also to those of modern oceanic rocks. This comparison is consistent with the conclusion obtained from the investigation on the clinopyroxenes of plutonic and volcanic rocks (SUN and BERTRAND, 1991).

Two magmatic suites are present in the YSPO. The suite I includes the whole plutonic sequence and the great majority of the volcanic rocks, whose trace element and REE concentrations are comparable to N-MORB. The suite II is only represented by the dykes II, which are characterized by the presence of Cpx phenocrysts. Their high LILE contents are comparable to the P-MORB or WPB.

The plutonic and suite I volcanic rocks are comagmatic, their parental magma has undergone an advanced fractionation at low pressure (< 5 kb). Using the 1-atm pseudo-quaternary Ol-Pl-Di-Q system, the formation ranges of the plutonics may be defined. The ultramafic cumulates were mainly precipitated in the Ol-volume. One part of the Mg-gabbros (troctolites and Ol-anorthosites) would have crystallized on the Ol-Pl bivariant cotectic surface and the other part (Ol-gabbros), on the Ol-Pl-Cpx univariant cotectic curve. The gabbronorites would have been formed at the Ol-Pl-Cpx-Opx invariant reaction point, and the ferrogabbros on the Pl-Cpx-Opx univariant cotectic curve. The Fe- and Ti-enrichment could take place at the Ol-Pl-Cpx-Opx reaction point. The albitites could have been formed after the precipitation of Ti-Mt.

The suite I volcanics represent the progressively evolved liquid in equilibrium with the cumulus phases of the plutonic rocks. Using $K_D^{ol-liq} = 0.30$ and $K_D^{cpx-liq} = 0.27$, the correspondence between plutonic and volcanic rocks can be established. The great majority of the volcanics might correspond to the magma on the Ol-Pl cotectic surface and Ol-Pl-Cpx cotectic curve, from which the Mg-gabbros would have precipitated. The ferrobasalts might correspond to the magma of the gabbronorites and ferrogabbros, and the keratophyres to the albitites in the plutonic sequence.

The suite I magma might have been derived from a slightly depleted mantle by a melting of about 15%, and submitted later to a low-pressure fractionation (< 5 kb), whereas the suite II magma might have been derived from an enriched mantle, also by about 15% partial melting, then undergoing a relatively high pressure fractionation (> 5 kb). Neither of these two magma suites corresponds to the liquid extracted from the studied mantle-derived peridotites.

The very advanced fractionation of the suite I magma, the coexistence of N-MORB (suite I) with P-MORB (suite II), and the abundant sills and sediments situated in the lower part of the volcanic section suggest that the YSPO began to form in small incipient oceanic basin(s). The basin(s) were generated by the break-up of an ancient continent (Archean to Early Proterozoic),

and could have developed towards a more mature stage like some sites on the East Pacific Rise and the Galápagos spreading center. The possible localities might be either the hot-spot-influenced spreading ridges in the vicinity of transform faults or directly in the latter, such as the Galápagos spreading center and some segments on the East pacific Rise.

The close similarity in petrography, geochemistry, mineralogy, and petrogenesis of YSPO to those of typical Phanerozoic high-Ti ophiolites and even to some present-day oceanic rocks indicates that the modern plate-tectonic processes would have been in operation since Middle Proterozoic time. The elucidation of the YSPO provides a good clue for the comprehension of the geological evolution history of the Yanbian-Shimian Proterozoic orogenic belt, or on a larger scale, the "Jinning Orogenic belt" (term used in the Chinese literature) on the western rim of the Yangtse Craton.

References

AGRELL, S.O. (1939): The adinoles of Dinas Head, Cornwall. Miner. Mag. 25, 305–337.

ALABASTER, T., PEARCE, J.A. and MALPAS, J. (1982): The volcanic stratigraphy and petrogenesis of the Oman ophiolite complex. Contrib. Mineral. Petrol., 81, 168–183.

ALLEGRE, C.J., TREUIL, M., MINSTER, J.F., MINSTER, B. and ALBAREDE, F. (1977): Systematic use of trace element in igneous process. Part I: Fractional crystallization processes in volcanic suites. Contrib. Mineral. Petrol., 60, 57–75.

ALLEGRE, C.J. and MINSTER, J.F. (1978): Quantitative models of trace element behavior in magmatic processes. Earth Planet. Sci. Lett., 38, 1–25.

ALTHERR, R., HENJES-KUNST, F., PUCHELT, H. and BAU-

MANN, A. (1988): Volcanic activity in the Red Sea axial trough. Evidence for a large mantle diapir. Tectonophysics, 150, 122–133.

BALLARD, R.D., HOLCOMB, R.T. and VAN ANDEL, T.H. (1979): The Galápagos rift at 86° W, 3. Sheeted flows, collapse pits, and lava lakes of the rift valley. J. Geophys. Res., 84, 5404–5422.

BEBIEN, J., OHNENSTETTER, D., OHNENSTETTER, M., PAUPY, A. and ROCCI, G. (1975): The role of hypabyssal magmatic rocks in our understanding of ophiolite model. Pétrologie, 1, 157–178.

BEBIEN, J., OHNENSTETTER, D., OHNENSTETTER, M. and VERGELY, P. (1980): Diversity of the Greek ophiolites: birth of oceanic basin in transcurrent systems. Ofioliti, 2, 129–198.

BEBIEN, J., BAROZ, F., CAPEDRI S. and VENTURELLI, G. (1987): Magmatismes basiques associés à l'ouverture d'un bassin marginal dans les Hellénides internes au Jurassique. Ofioliti, 12, 53–70.

BECCALUVA, L., OHNENSTETTER, D. and OHNENSTETTER, M. (1979): Geochemical discrimination between ocean floor and island arc tholeiites: application to some ophiolites. Can. J. Earth Sci., 16, 1874–1884.

BECCALUVA, L., PICCARDO, G.B. and SERRI, G. (1980): Petrology of Northern Apennine ophiolites and comparison with other Tethyan ophiolites. In: PANAYIOTOU, A. (ed.). Ophiolites: Proc. Int. Ophiolite Symp., Cyprus, 1979, 314–331.

BERHE, S.M. (1990): Ophiolites in Northeast and East Africa: implications for Proterozoic crustal growth. J. Geol. Soc. London, 147, 41–57.

BENDER, J.F., HODGES, F.N. and BENCE, A.E. (1978): Petrogenesis of basalts from the project FAMOUS area: experimental study from 0 to 15 kbars. Earth Planet. Sci. Lett., 41, 277–302.

BERTRAND, J., DIETRICH, V., NIEVERGELT, P. and VUAGNAT, M. (1987): Comparative major and trace element geochemistry of gabbroic and volcanic rock sequences, Montgenèvre ophiolite, Western Alps. Bull. suisse Minéral. Pétrogr., 67, 147–169.

BERTRAND, J., COURTIN, B. and VUAGNAT, M. (1982): Elaboration d'un secteur de lithosphère océanique liguro-piémontais d'après les données de l'ophiolite du Montgenèvre (Hautes Alpes, France et Province du Turin, Italie). Ofioliti, 7, 155–196.

BODINIER, J.L., DUPUY, C. and DOSTAL, J. (1984): Geochemistry of Precambrian ophiolites from Bou Azzer, Marocco. Contrib. Mineral. Petrol., 87, 43–50.

BONATTI, E. and MICHAEL, P.J. (1989): Mantle peridotites from continental rift to ocean basins to subduction zones. Earth Planet. Sci. Lett., 91, 297–311.

BRYAN, W.B. (1983): Systematics of modal phenocryst assemblages in submarine basalts: petrologic implication. Contrib. Mineral. Petrol., 83, 62–74.

BRYAN, W.B., THOMPSON, G., FREY F.A. and DICKEY, J.S. (1976): Inferred geological setting and differentiation in basalts from the Deep-Sea Drilling Project. J. Geophys. Res., 81, 4285–4303.

BRYAN, W.B. JUTEAU, T., ADAMSON, A.C., AUTIO, L.K., BECKER, K., BINA, M.M., EISSEN, J.P., FUJII, T. and GROVE, T.L. (1988): Deep-Sea Drilling Program Mid-Atlantic Ridge. Leg 106 and Leg 109, Site 648. Proc. Ocean Drill. Program., Part A 106, 109, 163–174.

BYERLY, G. (1980): The nature of differentiation trends in some volcanic rocks from the Galápagos spreading centre. J. Geophys. Res., 85, 3797–3810.

BYERLY, G., MELSON, W.G. and VOGT, P.R. (1976): Rhyodacites, andesites, ferro-basalts and ocean tholeiites from the Galápagos spreading centre. Earth Planet. Sci. Lett., 30, 215–221.

BYERS, C.D., CARCIA, M.O. and MUENOW, D.W. (1986): Volatiles in basaltic glasses from the East Pacific Rise at 21° N: implications for MORB sources and submarine lava flow morphology. Earth Planet. Sci. Lett., 79, 9–12.

CAMPSIE, J., JOHNSON, G.L., RASMUSSEN, M.H. and LAURSEN, J.L. (1984): Dredged basalts from the western Nazca plate and the evolution of the East Pacific Rise. Earth Planet. Sci. Lett., 68, 271–285.

CHEN, Q. and WANG, P. (1987): Polycycle activities of Panzhihua-Xichang paleo-rift: significance for its deep structure. J. Changchun College of Geology (Changchun Dizhi Xueyuan Xuebao), 17, 1–19 (in Chinese with English abstract).

CHRISTIE, D.M. and SINTON, J.M. (1986): Major element constraints on melting, differentiation and mixing of magma from Galápagos 95.5° propagating rift system. Contrib. Mineral. Petrol., 94, 274–288.

CHURCH, W.R. and RICCIO, L. (1977): Fractionation trends in the Bay of Island ophiolites of Newfoundland: polycyclic cumulate sequences in ophiolites and their classification. Can. J. Earth Sci., 14, 1156–1165.

CLAGUE, D.A. and BUNCH, T.E. (1976): Formation of ferrobasalts at East Pacific Mid-ocean Spreading Centers. J. Geophys. Res., 81, 4247–4256.

CLAGUE D.A., FREY, F.A. THOMPSON, G. and RINDGE, S. (1981): Minor and trace element geochemistry of oceanic rocks dredged from Galápagos spreading centre: role of crystal fractionation and mantle heterogeneity. J. Geophys. Res., 86, 9469–9482.

COISH, R.A. and CHURCH, W.R. (1979): Igneous geochemistry of mafic rocks in Betts Cove ophiolite, Newfoundland. Contrib. Mineral. Petrol., 70, 29–39.

COLEMAN, R.G. (1977): Ophiolites. Springer-Verlag, New York.

COLEMAN, R.G. (1984): Preaccretion tectonics and metamorphism of ophiolites. Ofioliti, 9, 205–222.

COLEMAN, R.G. and PETERMAN, Z.E. (1975): Oceanic plagiogranites. J. Geophys. Res., 80, 1099–1108.

COLEMAN, R.G. and McGUIRE, A.V. (1988): Magma system related to the Red Sea opening. Tectonophysics, 150, 77–100.

DANN, J.C. (1991): Early Proterozoic ophiolite, Central Arizona. Geology, 19, 590–593.

DIXON, S. and RUTHERFORD, M. (1979): Plagiogranites as late-stage immiscible liquids in ophiolite and midocean ridge suites: an experimental study. Earth Planet. Sci. Lett., 45, 45–60.

DIXON S. and RUTHERFORD, M. (1982): The origin of rhyolite and plagiogranite in oceanic crust: an experimental study. J. Petrol., 24, 1–25.

ELTHON, D. (1991): Geochemical evidence for formation of the Bay of islands ophiolite above a subduction zone. Nature, 354, 140–142.

ENGEL, C.G. and FISHER, R.L. (1975): Granitic to ultramafic rock complexes of the Indian Ocean Ridge system, Western Indian Ocean. Geol. Soc. Am. Bull., 86, 1153–1178.

FLOYD, F.A, KELLING, G., GÖKCEN, S.L. and GÖKCEN, N. (1991): Geochemistry and tectonic environment of basaltic rocks from the Misis ophiolitic mélange, south Turkey. Chem. Geol., 89, 263–279.

FREY, F.A., GREEN, H.D. and ROY, S.D. (1978): Integrated models of basalt petrogenesis: a study of quartz tholeiites to olivine melilitites from south eastern Australia utilizing geochemical and experimental data. J. Petrol., 19, 463–513.

GEOLOGICAL TEAM 106 (1975): Pre-sinian geological feature of Middle section of Kan dian axis and its relationship to plate tectonics. Scientia Geologica (Dizhi Kexue), No. 2, 107–113 (in Chinese with English abstract).

GILL, J.B. (1981): Orogenic andesites and plate tectonics. Springer-Verlag, Berlin, Heidelberg, New York.

GROVE, T.L. and BRYAN, W.B. (1983): Fractionation of pyroxene-phyric MORB at low pressure: an experimental study. Contrib. Mineral. Petrol., 84, 293–309.

GROVE, T.L. and BAKER, M.B. (1984): Phase equilibrium of the tholeiitic versus calc-alkaline differentiation trends. J. Geophys. Res., 89, 3253–3274.

HARPER, G.D. (1985): Archean ophiolites, Wind River Mountains Wyoming (USA). Ofioliti, 10, 297–236.

HEBERT, R., BIDEAU, D. and HEKINIAN, R. (1983): Ultramafic and mafic rocks from the Garret transform fault near 13°30' S on the East Pacific Rise: igneous petrology. Earth Planet. Sci. Lett., 65, 107–125.

HEKINIAN, R. and THOMPSON, G. (1976): Comparative geochemistry of volcanics from rift valley, transform faults and aseismic ridges. Contrib. Mineral. Petrol., 57, 145–162.

HEKINIAN, R., MOORE, J.G. and BRYAN, W.B. (1976): Volcanic rocks and processes of the Mid-Atlantic Ridge rift valley near 36°47' N. Contrib. Mineral. Petrol., 58, 83–110.

HOFMANN, A.W. (1988): Chemical differentiation of the earth: the relationship between mantle, continental crust, and oceanic crust. Earth Planet. Sci. Lett., 90, 297–314.

IMSLAND, P. (1983): Iceland and ocean floor: comparison of chemical characteristics of the magmatic rocks and some volcanic features. Contrib. Mineral. Petrol., 83, 31–37.

IKEDA, Y. (1990): CeN/SrN/SmN: A trace element discriminant for basaltic rocks from different tectonomagmatic environments. N. Jb. Mineral. Mh, H.4, 145–158.

ISHIWATARI, A. (1985): Igneous petrogenesis of the Yakuno ophiolite (Japan) in the context of the diversity of ophiolites. Contrib. Mineral. Petrol., 89, 155–167.

JAHN, B.-M. (1986): Mid-ocean ridge or marginal basin origin of the Taiwan ophiolite: chemical and isotopic evidence. Contrib. Mineral. Petrol., 92, 194–206.

JACQUWS, A.L. and GREEN, D.H. (1980): Anhydrous melting of peridotite at 0–15 kb pressure and the genesis of tholeiitic basalts. Contrib. Mineral. Petrol., 73, 287–310.

JUTEAU, T., NOACK, Y. and WHITECHURCH, H. (1980): Mineralogy and geochemistry of alteration products in Holes 417A and 417D basement samples (Deep Sea Drilling Project). Initial Repts. D.S.D.P., 51, 52, 53, 1273–1297.

KAY, R.W. and SENECHAL, R.G. (1976): The rare earth geochemistry of the Troodos ophiolitic complex. J. Geophys. Res., 81, 964–970.

KENNEDY, A.K., GROVE, T.L. and JOHNSON, R.W. (1990): Experimental and major element constraints on the evolution of lavas from Lihir Island, Papua New Guinea. Contrib. Mineral. Petrol., 104, 722–734.

KONTINEN, A. (1987): An early Proterozoic ophiolite, the Jormua mafic-ultramafic complex, Northeastern Finland. Precambrian Res., 35, 313–341.

LAI, M.Z. (1983): The geochemical feature of the Yanbian pre-sinian ophiolite. In: Panxi Geological Brigade (ed.). Panxi Geology, 1, 35–54 (in Chinese).

LAURENT, R. and HEBERT, R. (1989): The volcanic and intrusive rocks of Québec Appalachian ophiolites (Canada) and their island-arc setting. Chem. Geol., 77, 287–302.

LE BAS, M.J., LE MAITRE, R.W., STRECKEISEN, A. and

ZANETTIN, B. (1986): A chemical classification of volcanic rocks based on the Total Alkali-Silica Diagramme. J. Petrol., 27, 745–750.

LEBLANC, M. (1976): A Proterozoic ocean crust at Bou Azzer. Nature, 216, 34–35.

LE ROEX, A.P., DICK, H.J.B., ERLANK, A.J. and REID, A.M. (1983): Geochemistry, mineralogy and petrogenesis of lavas erupted along the Southwest Indian Ridge between the Bouvet Triple Junction and 11 degrees east. J. Petrol., 24, 267–318.

LE ROEX, A.P., DICK, H.J.B., REID, A.M., FREY, F.A., ERLANK, A.J. and HART, S.R. (1985): Petrology and geochemistry of basalts from the American-Atlantic Ridge, Southern Ocean: implications from the westward influence of the Bouvet mantle plume. Contrib. Mineral. Petrol., 90, 367–380.

LEWIS, A.D. and SMEWING, J.D. (1980): The Montgenèvre ophiolite (Hautes Alpes, France): metamorphism and trace element geochemistry of the volcanic sequence. Chem. Geol., 28, 291–306.

LI, J.L. (1984): Eugeosyncline rock association of Yanbian Group in Western Sichuan, China. Bull. Chinese Acad. Geol. Sci. (Zhongguo Dizhikexueyuan Yuanbao), 8, 31–37 (in Chinese).

LI, J.L., ZHANG, F.Q. and WANG, S.X. (1983): Characteristics of REE distribution of Yanbian Proterozoic ophiolite, Sichuan Petrol. Research (Yanshixue Yanjiu), 3, 37–43 (in Chinese).

LUO Y.N. (1983): The evolution of the paleo-plate tectonics of the Kandian structural zone. Earth Sciences (Diqiu Kexue), 3, 93–101 (in Chinese).

LUO, Y.N. (1988): Geological settings of formation of the Panxi paleo-rift. In: Zhang, Y.X. (ed.). The geological and tectonic features of the Panzhihua-Xichang rift. Publishing House of Geology, Beijing, China, 7–34 (in Chinese).

MARCHAL, M. and OHNENSTETTER, D. (1984): The ophra data bank. Ofioliti. 9, 633–676.

MERCIER, J.C. and NICOLAS, A. (1975): Texture and fabrics of upper mantle peridotites as illustrated by xenoliths from basalts. J. Petrol., 16, 454–487.

MEVEL C. (1975): Les zones chimiques dans les pillow-lavas spilitiques du Chenaillet et des Gets (Alpes françaises). Pétrologie, I, 313–333.

MINSTER, J.F. and ALLEGRE, C.J. (1978): Systematic use of trace element in igneous processes. Part II: inverse problem of batch partial melting in volcanic suites. Contrib. Mineral. Petrol., 68, 37–52.

MIYASHIRO, A. (1973a): Metamorphism and metamorphic belts. George Allen and Unwin, London, 472 pp.

MIYASHIRO, A. (1973b): Troodos ophiolitic complex was probably formed in an island arc. Earth Planet. Sci. Lett., 19, 218–224.

MIYASHIRO, A. (1974): Volcanic rock series in island arcs and active continental margins. Am. J. Sci., 274, 321–355.

MIYASHIRO, A. (1975): Classification, characteristics and origin of ophiolites. J. Geol., 83, 249–281.

MIYASHIRO, A. and SHIDO, F. (1980): Differentiation of gabbros in the Mid-Atlantic Ridge near 24° N. Geochem. J., 14, 146–156.

MULLEN, E.O. (1983): $MnO/TiO_2/P_2O_5$: a minor element discrimination for basaltic rocks of oceanic environments and its implications for petrogenesis. Earth Planet. Sci. Lett., 62, 53–62.

MYSEN, B. and KUSHIRO, I. (1977): Compositional variations of coexisting phases with degree of melting of peridotite in the upper mantle. Amer. Mineral., 62, 843–865.

NAKAMURA, N. (1974): Determination of REE, Ba, Fe, Mg, Na, and K in carbonaceous and ordinary chondrites. Geochim. Cosmochim. Acta, 38, 757–775.

NICOLAS, A., BOUDIER, F. and BOUCHEZ, J.-L. (1980): Interpretation of peridotite structures from ophiolitic and oceanic environments. Am. J. Sci., 280A, 192–210.

NIELSON, P.J.E. and SCHWARZMAN, E.C. (1976): Classification of textures in ultramafic xenoliths. J. Geol., 85, 49–61.

OHNENSTETTER D. and OHNENSTETTER, M. (1975): Le puzzle ophiolitique corse. Un bel exemple de paléo-dorsale océanique. Thèse 3e cycle, Nancy, 418.

OHNENSTETTER, D. and OHNENSTETTER, M. (1980): Ophiolitic sequences in Corsica. Ofioliti, 1, 53–58.

PEARCE, J.A. (1975): Basalt geochemistry used to investigate past tectonic environments on Cyprus. Tectonophysics, 25, 42–67.

PEARCE, J.A. (1980): Geochemical evidence for the genesis and eruptive setting of lavas from the Tethyan ophiolites. In: PANAYIOTOU (ed.). Ophiolites: Proc. Int. Ophiolite Symp., Cyprus, 1979, 261–272.

PEARCE, J.A. (1991): Ocean floor comes ashore. Nature, 354, 110–111.

PEARCE, J.A. and CANN, J.R. (1973): Tectonic setting of basic volcanic rocks determined using trace element analyses. Earth Planet. Sci. Lett., 19, 290–300.

PEARCE, J.A. and NORRY, M.J. (1979): Petrogenetic implication of Ti, Zr, Y, and Nb variations in volcanic rocks. Contrib. Mineral. Petrol., 69, 33–47.

PEARCE, J.A., LIPPARD, S.J. and ROBERTS, S. (1984): Characteristics and tectonic significance of supra-subduction zone ophiolites. Geol. Soc. Lond. Spec. Publ., 16, 77–94.

PEARCE, J.A., ROGERS, N., TINDLE, A.J. and WATSON, J.S. (1986): Geochemistry and petrogenesis of basalts from Deep Sea Drilling Project Leg 92, Eastern Pacific. Initial Repts. D.S.D.P., 92, 435–497.

POGNANTE, U., LOMBARDO, B. and VENTURELLI, G. (1982): Petrology and geochemistry of Fe–Ti gabbros and plagiogranites from the Western Alps ophiolites. Bull. suisse Minéral. Pétrogr., 62, 457–472.

PRESNALL, D.C., SELENA, A., DIXON, J.R., DIXON, T.H., O'DONNELL, N.L., BRENNER, R.L., SCHROCK, R.L. and DYCUS, D.W. (1978): Liquidus phase relation on the joint diopside-forsterite-anorthite from 1 atm to 20 bar: their bearing on the generation and crystallization of basaltic magma. Contrib. Mineral. Petrol., 66, 203-220.

PRESNALL, D.C., DIXON, J.R., O'DONNELL, T.H. and DIXON, S.A. (1979): Generation of mid-ocean ridge tholeiites. J. Petrol., 20, 3–35.

ROEDER, P.L. and EMSLIE, E.F. (1970): Olivine-liquid equilibrium. Contrib. Mineral. Petrol., 29, 275–289.

SAUNDERS, A.D., FORNARI, D.J. and MORRISON, M.A. (1982): The composition and emplacement of basaltic magmas during the development of continental-margin basin: the Gulf of California, Mexico. J. Geol. Soc. London, 139, 335–346.

SCHILLING, J.-G. (1975): Rare-earth variation across "normal segment" of the Reykjanes Ridge, 60°–53° N, Mid-Atlantic Ridge, 29° S, and East Pacific Rise, 2°–19° S, and evidence on the composition of the underlying low-volocity layer. J. Geophys. Res., 82, 4285–4304.

SCHILLING, J.-G., KINGSLEY, R.H. and DEVINE, J.D. (1982): Galápagos hotspot-spreading center system, 1. Spatial petrological and geochemical variations (83° W –101° W). J. Geophys. Res., 87, 5593–5610.

SERRI, G. (1980): Chemistry and petrology of gabbroic complexes from Northern Apennine ophiolites. In:

Panayiotou (ed.). Ophiolites: Proc. Int. Ophiolite Symp., Cyprus, 1979, 296–313.

SERRI, G. (1981): The petrogeochemistry of ophiolite gabbroic complexes: a key to the classification of ophiolites into low-Ti and high-Ti type. Earth Planet. Sci. Lett., 52, 203–212.

SERRI, G. and SAITTA, M. (1980): Fractionation trends of the gabbroic complexes from high-Ti and low-Ti ophiolites and the crust of major oceanic basin: a comparison. Ofioliti, 5, 241–268.

SHAW, D.M. (1970): Trace element fractionation during anataxis. Geochim. Cosmochim. Acta, 34, 237–243.

SHERVAIS, J.W. (1982): Ti-V plots and petrogenesis of modern and ophiolitic lavas. Earth Planet. Sci. Lett., 59, 101–118.

STOLPER E. (1980): A phase diagram for Mid-Ocean Ridge basalts: preliminary results and implications for petrogenesis. Contrib. Mineral. Petrol., 74, 13–28.

SUN, C.M. (1990): Ophiolites riches en Ti du protérozoïque près de Shimian et de Yanbian dans la Province du Sichuan en Chine. C. R. Acad. Sci. Paris, t. 30, Série II, 1673–1679.

SUN, C.M. and BERTRAND, J. (1991): Geochemistry of clinopyroxenes in plutonic and volcanic sequences from the Yanbian Proterozoic ophiolites (Sichuan Province, China): petrogenetic and geotectonic implications. Bull. suisse Minéral. Pétrogr. 71, 243–259.

SUN, S.-S. (1982): Chemical composition and origin of the earth's primitive mantle. Geochim. Cosmochim. Acta, 46, 179–192.

SUN, S.-S., NESBITT, R.W. and SHARASKIN, A.Y. (1979): Geochemical characteristics of Mid-ocean ridge basalts. Earth Planet. Sci. Lett., 44, 119–138.

VENTURELLI, G., CAPEDRI, S., THORPE, S. and POTTS, P.J. (1979): Rare-earth and other element distribution in some ophiolitic metabasalts of Corsica, Western Mediterranean. Chem. Geol., 24, 339–353.

VUAGNAT, M. (1946): Sur quelques diabases suisses: contribution à l'étude des spilites et des pillows lavas. Bull. suisse Mineral. Pétrogr., 26, 116–228.

VUAGNAT, M. (1952): Sur une structure nouvelle observée dans les roches vertes du Montgenèvre (Hautes-Alpes). Arch. Sci. Genève, 5, 191–193.

VUAGNAT, M. (1953): Sur un phénomène de métasomatisme dans les roches vertes du Montgenèvre (Hautes-Alpes). Bull. Soc. franç. Minéral. Crist., 76, 438–450.

VUAGNAT, M. (1954): Sur les ophisphérites de la région des Gets (Haute-Savoie). Arch. Sci. Genève, 7, 5–14.

WALKER, D., SHIBATA, T. and DELONG, S.E. (1979): Abyssal tholeiites from the Oceanographer Fracture Zone II, phase equilibria and mixing. Contrib. Mineral. Petrol., 70, 111–125.

WOOD, D.A. (1978): Major and trace element variation in the tertiary lavas of Eastern Iceland and their significance with respect to the Iceland geochemical anomaly. J. Petrology, 19, 397–436.

YANG, T. and JIANG, X.D. (1988): Reevaluation of the Panzhihua layered ore-bearing complex, China. J. Changchun College Geol. (Changchun Dizhi Xueyuan Xuebao), 18, 125-136 (in Chinese with English abstract).

YUAN, H.H., ZHANG, S.F. and ZHANG, P. (1985): Isotopic geochronology of Panzhihua-Xichang area: research report (in Chinese, unpublished).

ZEN, X.J. (1985): The geochemistry of the Yanbian Group volcanic rocks: Research report (in Chinese, unpublished).

ZEN, X.J., XU, X.Z., YANG, Q.W. and YUAN, L.P. (1982): The ultramafic and mafic bodies of Shimian – probably a dismembered Proterozoic ophiolite. In: Panxi Geological brigade (ed.). Research report on the Candian paleo-rift belt, 24-36 (in Chinese).

ZHANG, Z.M., LIOU, J.G. and COLEMAN, R.C. (1984): An outline of the plate tectonics of China. Geology, 95, 295–312.